

Liquid Crystals - Decision on Manuscript ID TLCT-2019-0054.R1

From: Liquid Crystals (onbehalf@manuscriptcentral.com)

To: dakshinamurthy_potukuchi@yahoo.com

Date: Sunday, 21 July, 2019, 08:53 pm IST

21-Jul-2019

Dear Professor Potukuchi

Your manuscript entitled "Influence of Meta-Extended Rigid-Core, Complementary Hydrogen Bonding and Flexible Chain on Polymorphism in Schiff-based Hydrogen Bonded Liquid Crystals: (4)MeOBD(3)AmnBA:nOBAs" which you submitted to Liquid Crystals, has been reviewed. The reviewer's comments are included at the bottom of this letter.

The review is favourable and suggests that, subject to minor revisions, your paper is suitable for publication. Please consider these suggestions, and I look forward to receiving your revision.

It is also very important that the reference style used in your manuscript is consistent with the Journal's. The Publishers have been reviewing the reference style for Liquid Crystals to ensure that it matches industry standards. For the journal to stay competitive we need to keep up with advances in typesetting technology, third party indexing and reference validation, leading to a better quality of article and a better service to authors. From 2013, the style adopted by the Journal is described at: http://www.tandf.co.uk/journals/authors/style/reference/tf_NLM.pdf. The new style (NLM) is supported by EndNote. For a Journal article the reference style is:

Author AA, Author BB, Author CC. Title of article.
Abbreviated Journal Title. 2012;62:112–116.

Please reformat your manuscript to comply with this style. If you have not done this correctly, your manuscript will be returned to you and publication could be delayed.

When you revise your manuscript please highlight the changes you make in the manuscript by using the track changes mode in MS Word or by using bold or coloured text.

To submit the revision, log into <https://mc.manuscriptcentral.com/tlct> and enter your Author Centre, where you will find your manuscript title listed under "Manuscripts with Decisions." Under "Actions," click on "Create a Revision." Your manuscript number has been appended to denote a revision. Please enter your responses to the comments made by the reviewer(s) in the space provided. You can use this space to document any changes you made to the original manuscript. Please be as specific as possible in your response to the reviewer(s).

Alternatively, once you have revised your paper, it can be resubmitted to Liquid Crystals by way of the following link:

*** PLEASE NOTE: This is a two-step process. After clicking on the link, you will be directed to a webpage to confirm. ***

https://mc.manuscriptcentral.com/tlct?URL_MASK=1a8e928bc2c647b9a535a7d89ce35d5d

IMPORTANT: Your original files are available to you when you upload your revised manuscript. Please delete any redundant files before completing the submission.

The Publishers cannot work with PDF files to prepare the proofs of your paper and so it is essential that you upload all the source files for your manuscript and not the PDF file. If you do not do this the publication of your manuscript will be delayed.

Because we are trying to facilitate timely publication of manuscripts submitted to Liquid Crystals, your revised manuscript should be uploaded as soon as possible. If it is not possible for you to submit your revision in a reasonable amount of time, we may have to consider your paper as a new submission.

Once again, thank you for submitting your manuscript to Liquid Crystals and I look forward to receiving your revision.

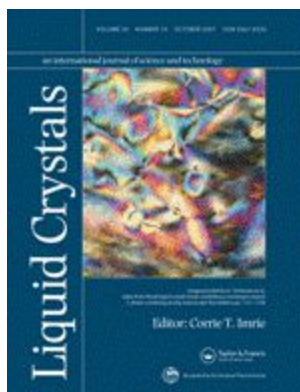
Yours sincerely
Professor Corrie Imrie
Editor, Liquid Crystals
c.t.imrie@abdn.ac.uk

Referee's Comments to Author:

The reviewer acknowledges the efforts made by the authors in this latter revision.
There are still minor aspects that should be addressed, including a detailed proof read of the next version, and possibly language polishing.
Some of these are flagged in the document attached, as comments in a pdf file.
Sincerely,



TLCT-2019-0054-R1 commented.pdf
5.7MB

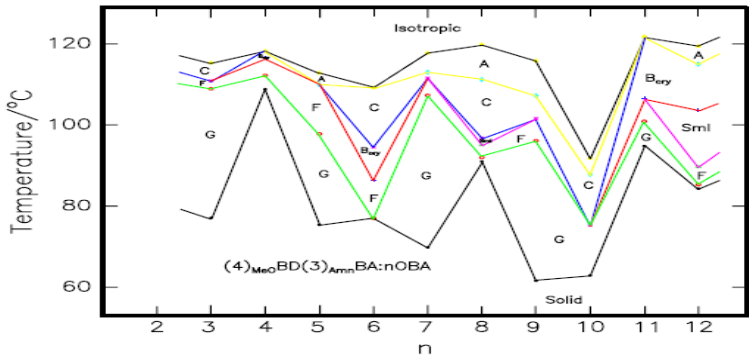
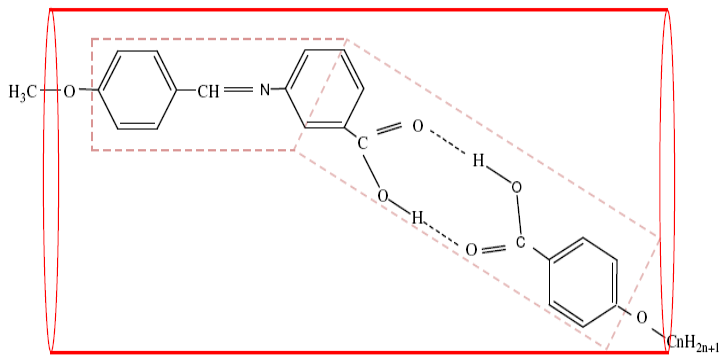


**Influence of Meta-Extended Rigid-Core, Complementary Hydrogen Bonding and Flexible Chain on Polymorphism in Schiff-based Hydrogen Bonded Liquid Crystals:
(4)MeOBD(3)AmnBA:nOBAs**

Journal:	<i>Liquid Crystals</i>
Manuscript ID	TLCT-2019-0054.R1
Manuscript Type:	Original Article
Date Submitted by the Author:	30-May-2019
Complete List of Authors:	AVSN, Krishna Murthy; Jawaharlal Nehru Technological University:Kakianda, Chemistry M, Srinivasulu; Manipal University, Chemistry Attaluri, Venkat Ashok; JNTUniversity:Kakinada, Physics Y, Venkateswar Rao; Jawaharlal Nehru Technological University:kakinada, Chemistry potukuchi, dakshina; JNTUniv. Kakinada, Physics
Keywords:	Schiff based moieties, Complementary Hydrogen Bonding, Transition temperatures, Odd-even effect, Enthalpy, Phase stability, Multi-critical point, Meata-extended core

SCHOLARONE™
Manuscripts

1
2
3
4
5
6
7
8
9
10
11
12
13
14
15
16
17
18
19
20
21
22
23
24
25
26
27
28
29
30
31
32
33
34
35
36
37
38
39
40
41
42
43
44
45
46
47



Influence of Meta-Extended Rigid-Core, Complementary Hydrogen Bonding and Flexible Chain on Polymorphism in Schiff-based Liquid Crystals: (4)_{MeO}BD(3)_{Am}BA:nOBAs

AVSN Krishna Murthy, [§]M.Srinivasulu, AVN Ashok Kumar, YV Rao and *DM Potukuchi

Faculty of Physical Sciences, University College of Engineering, Jawaharlal Nehru Technological University:Kakinada, Kakinada-533003, AP, India.

[§]Department of Chemistry, Manipal University of Higher Education, Manipal-576104, India.

Abstract

Schiff based complementary hydrogen bonded liquid crystals (HBLC), viz., (4)_{MeO}BD(3)_{Am}BA:nOBA's with flexible chain length for $n=3,4,5,6,7,8,9,10,11$ and 12 are reported. ¹H; ¹³C-NMR and Infra-Red spectroscopy used to confirm the formation of HBLCs. LC phases and transition temperatures (T_c) determined by polarized optical microscopy (POM) and differential scanning calorimetry (DSC). T_c and enthalpy (ΔH) determined by DSC also. Odd-even effect observed at clearing and melting transitions. Influence of Schiff base and Oxygen as bridging atom promote smectic phase abundance. HBLCs exhibit tetra- or penta-phase variance. Maximum (penta) phase variance is exhibited by $n=8$ and 12 with long flexible chain. Prevalent abundance of quasi-2dimensional (2D) LC phases SmF and SmI are observed. Nematic phase is quenched. Lower ($n=4$) and intermediate ($n=6$) members exhibited SmB_{cryst} phase. *Predominant occurrence of enantiotropic LC phases is noticed. All members exhibited 3D tilted SmG phase. AC transition exhibited by intermediate homologues (for $n=7, 8, 9$ and 10) is found to be either second order or with very small enthalpy. Phase diagram reveals the abundance of multi-critical points, some involving exotic symmetries. Influence of meta-extended rigid core, complementary HB and flexibility are studied for the LC phase abundance with characteristic structural order. POM and DSC results are discussed in the wake of reports in other achiral calamitic LCs.*

Keywords: Schiff based moieties; Complementary Hydrogen Bonding; Smectic liquid crystal phases, Transition temperatures; Enthalpy; Odd-even effect; Multi-critical point; Phase stability.

*Author for Correspondence: dakshinamurthy_potukuchi@yahoo.com

1. Introduction

Liquid Crystals (LC) possess dual [1] properties of isotropic fluids and anisotropic crystals. LC phase structures are interesting as they catered the awaited experimental proof [2,3] for the theoretical predictions of 1D-, 2D- and quasi 2D-crystal melting transitions and anisotropic scaling hypothesis. Recently, they are identified [4] to mimic the transitions of topological insulators. Inherent large birefringence and high contrast ratios along with the fluid nature exhibited by LC phase structures promoted [5,6] their utility in electro-optic (EO) devices. Interdisciplinary research activity by physicists and chemists in the area of LCs is targeted to realize ambient LC phase structures with large field response. LC physico-chemical research involves design and architectural aspects like chemical moieties, configuration, conjugation, chiral centers, interaction (bonding between moieties) etc., Design of calamitic [7] or rod-like, discotic [8], hydrogen bonded [9-12], bent [13], phasidic [14] etc., types of LCs are known to exhibit phases of structural diversity. Initially, Nematic LCs (or their structural analogues like cholesterics etc.,) are underlined by long range orientational order [7] are used in displays [15] operating with millisecond speed. Advent of ferroelectric response in chiral calamitic type of LCs stimulated [16] the LC synthetic research activity to realize the layered tilted smectic phases. Chiral versions of tilted smectic phases, SmC* are found to respond [6] at microsecond speed. Hence, realization of tilted smectic phases with wide temperature range and large tilt angle in the vicinity of ambient temperatures occupied the center stage of LC synthetic chemists.

Much of the LC molecular design reported [17,18] owes to the calamitic/rod type molecular structure. Details of chemical moieties (aliphatic/aromatic) used, viz., as rigid core [17,18], bridging (Oxygen atom) groups [18,19] and flexible chains [17,19-21], chemical bonding or interaction [9-12], configuration of polar substitutions [22-26], conjugated environment [17,22,27,28], ester moieties [16,17,22,25,29,30], aromatic moieties [17,19,26,30], Schiff based [17,19,25,31,32] moieties etc., on the molecular body are found to influence the stability and diversity of LC phases towards ambient temperatures. Involvement of hydrogen bonding (HB or soft-covalent) interaction [9-12] on the molecular frame of LC is known as the most effective way of growth of supra molecular (SM) assemblies. Design of HBLCs mediated by soft-covalent interaction and SM assembly of chemical moieties

accelerated the research activity. Selection of proton donor/acceptor moieties, direction of bonding (with respect to the molecular long axis) and bonding nature, i.e., being linear [10,32-35], complementary [9,24,36], alternative [37], double [38-40] types are also reported to influence the stability and diversity of LC phase structures. Presence of HB in LCs is found [9,10,24,28-31,36-40,41-42] to increase phase stability towards room temperature. Complementary type of HB is recognized [9,24,36,38-40,41-42] to enhance the rigidity component in calamitic type of LCs, and thereby to promote LC phase abundance. Inclined configuration of HB (to the molecule's longitudinal direction) is found [39] to enhance the transverse dipole moment μ_t and result for induction of tilted smectic phases. Additionally, the tilted smectic phase stability is found [36,39,40] to get depressed towards room temperatures along with growth of re-entrant SmC phase by the involvement of HB interaction in dimers. Intra-molecular hydrogen bonding is also reported [10] to influence mesomorphic stability. Phase stability is reported [11] to be influenced by the inclusion of HB in main chain, side chain and cross-linked polymeric liquid crystals also.

Continuous increasing of chain length (or flexible component by adding methylene $-\text{CH}_2-$ units) is found [17,19-21,43-45] to result for alternating trend of melting and clearing temperatures, known as odd-even (OE) effect. OE effect indirectly influences the LC phase stability and it is reported to be originated [44] by the alternating contributions of axial polarizabilities. Lateral substitutions [18,24,46] with highly polar substitutions ($-\text{C}\equiv\text{N}$, $-\text{F}$, $-\text{Cl}$, $-\text{Br}$, $-\text{NO}_2$, $-\text{NH}_2$ etc.), on the calamitic molecular frame are found to result for large Nematic phase stability. Increasing flexible end chain length is argued [47,48] to induce orientational disorder, which in turn promotes the stability of quasi-2D hexatic smectic phases (SmB_{Hex} , SmI , SmF) with bond-orientational order and exotic symmetries. Involving electro-negative Oxygen as bridging (between flexible chain and rigid core) atom is found [19,49] to promote lateral stacking and lead to the induction and stability of layered smectic phases. Bent type of molecular architecture is found [13,43,50,51-56] to result for ferro-electric (FE) response in achiral molecules also. Discotic molecular design is found [57,58] to result for semiconductor properties and thermoelectric response in LC phases.

Investigations for influence of design and architecture features of molecules capable of exhibiting LC phases of device interest are an ongoing topic of research.

Selection of O-atom as bridging moiety [22,23] and Schiff base [17,19,25,31,32] as core are known to promote lateral stacking and growth of layered smectic phases. HB interaction in LCs is found to be inclined with respect to the long molecular axis, which in turn has enhanced device savvy tilted smectic phase stability. Despite the achiral constitution, B₂ and B₅ phases of bent shaped LCs are known [13,28,50] to exhibit ferroelectric response. In calamitic type of LC molecules, a meta-positioned extension is anticipated to result for enhanced μ_t and impart slightly bent shape for the possible enhancement of device savvy tilted phase abundance. In the wake of the expected influence of molecular (Figure-1) design (or architectural features by proper [7-19] selection of chemical moieties) for the growth of device savvy LC phases, an attempt is made to design a series of calamitic type of achiral LCs possessing

- i) soft-covalent (HB) interaction,
 - ii) Schiff based moieties,
 - iii) electron releasing lateral substitutions and
 - iv) meta-extended rigid core
- in anticipation of enhanced tilted smectic phases.

An indigenously synthesized series of calamitic type of LCs possessing complementary HB comprised of meta extended core are investigated by nuclear magnetic resonance (NMR) and Fourier-Transform Infrared (FTIR) spectroscopy techniques to confirm their formation. LC phase structures and phase transition temperatures (T_c) are determined [59,60] with the help of polarized optical spectroscopy (POM). Phase transition temperatures and heats of transition (enthalpy ΔH) associated with LC phases are also determined by differential scanning calorimetry (DSC). Total LC phase stability $[\Delta T]_{LC}$, SmC phase stability $[\Delta T]_C$ and overall tilted phase stability $[\Delta T]_{Tilt}$ is estimated by evaluating the difference between clearing and melting temperatures of the phase of interest. However, $[\Delta T]_{Tilt}$ includes the data for all the tilted LC phase thermal stabilities viz., SmC, SmI, SmF, and SmG. Paper is organized in 3-sections comprised of introduction, details of experimental techniques, synthetic route and discussion of results.

2. Experimental Methods and Synthesis

2a. Experimental Techniques

A Bruker - Avance NMR spectrometer is used to record ^1H -NMR spectra (300 MHz) and ^{13}C -NMR spectra (75 MHz) for the identification [61,62] and tally of H-atoms (Figure-2 as representative) and C-atoms (Figure-3 as representative) positioned at various places of the targeted of HBLC complex. The presence of HB is identified [63] with solid state (KBr pellet) FTIR spectra (ABB Bomem) at room temperature and analyzed with MB3000 software. FTIR spectra is analyzed in the backdrop of reports [64-68] on supra-molecular LCs possessing HB interaction, viz., in aromatic/aliphatic acids, nOBAs and Schiff base compounds involving $>\text{C}=\text{O}$, $-\text{OH}$ stretching and Fermi resonance of A-, B- and C-bands. POM textures [59,60] are recorded and analyzed with the help under programmed heating/cooling mode at a rate of $0.1^\circ\text{C}/\text{min}$. LC samples targeted for POM study are prepared as microscopic slides (through rubbing technique). POM studies are carried out over homogeneously aligned sample also by introducing the sample into the Device Tech (USA) made polyimide buffed thin transparent glass cells of $5\ \mu\text{m}$ thickness. Thustextural observations of LC phase structures are carried out using an SD Tech POM equipped with Charged Coupled Device (CCD) camera and μ -master software in conjunction with an INSTEC 402 hot stage (STC 200 heating system). Phase transition temperatures recorded with POM technique are accurate to $\pm 0.1^\circ\text{C}$. A Shimadzu DSC-60 differential scanning calorimeter is used to determine the LC phase transition temperatures ($\pm 0.1^\circ\text{C}$) and the heat (ΔH , at $\pm 0.01\text{J/g}$) of transition. The cooling and heating rates adopted during the DSC are $5^\circ\text{C}/\text{min}$.

2b. Synthesis

The chemical reactants, viz., mesogenic p-n-alkoxy benzoic acids (nOBA's), p-methoxybenzaldehyde and m-aminobenzoic acid are procured from Sigma Aldrich (USA). Solvents of AR grade, viz., tetrahydrofuran (THF), glacial acetic acid and ethyl alcohol are procured from CDH (India).

The three-step synthetic path followed during the preparation of targeted HBLC series is presented in Scheme-1. In the first step, p-methoxybenzaldehyde and m-amino benzoic acid were mixed in equi-molar ratio (1:1) in ethanol at cold conditions. 4-5 drops of glacial acetic acid is added to enhance the yield of Schiff based intermediate compound in the condensation reaction. Intermediate product, viz., 3-(4-methoxybenzylideneamino)benzoic acid is isolated from solvent by filtration under reduced pressure conditions. The product obtained in the 1st step is found to

be colourless which signifies its initial purity and susceptibility against possible chemical degradation. In the **second** step, the dimeric forms of nOBAs (for $n=3$ to 12) were converted to monomer form by dissolving in THF. In the **third** step, each monomer form of nOBA is mixed with 3-(4-methoxybenzylideneamino) benzoic acid in 1:1 molar ratio in excess amount of THF and the reactants are refluxed for 5 hours. Solvent is removed after the formation of HBLC complex under reduced pressure conditions. The general molecular formula for the final product HBLC complex is given as $(4)_{MeO}BD(3)_{Am}BA:nOBA$.

3. Results and Discussion

3a. Supra-Molecular Structure of HBLC complexes

Supra-molecular structure (Figure-4) of the targeted HBLC compound constituted by HB interaction and meta-position extended rigid core part is presented in scheme-1. An overview of HBLC seems to entail a rigid core constituted by a Schiff base (possessing meta-situated acid) interacted through HB with an aromatic acid ($-COOH$ of nOBA). Overview of the molecular structure reveals that one of flexible ends contains Oxygen as bridging atom. As O-atom is highly electro-negative, it is anticipated to promote lateral stacking [22] to pronounce smectic phase abundance. It is also noticed that Schiff based acid $(4)_{MeO}BD(3)_{Am}BA$ and nOBA along with the HB interacted space (on the molecular frame) provide the essential rigidity to the LC molecule. However, length of end chain ($-CH_2$ units in nOBA) is varied to tune the flexibility for the possible induction of orientational disorder.

3b. FTIR Spectra

Presence of HB interaction in the meta extended HBLC complexes is investigated by FTIR study. The FTIR spectra of $(4)_{MeO}BD(3)_{Am}BA:5OBA$ (as representative) as augmented by the spectra for 5OBA and schiff based intermediate are presented in Figures-5_{a,b,c}. IR spectra of chemical components carboxylic acid i.e., 5OBA and intermediate Schiff's base, viz., $(4)_{MeO}BD(3)_{Am}BA$ are also presented in the same figure for comparative analysis. The data for prominent IR absorptions characteristic underlying functional groups is presented in Table-1.

The FTIR spectrum of $(4)_{MeO}BD(3)_{Am}BA$ exhibited strong absorption peaks at 2931 and 2869 cm^{-1} which correspond to the C-H stretching. A shoulder at 3062 cm^{-1} is identified to correspond to the fundamental mode of vibration of hydroxyl ($-OH$) group of the carboxylic acid. It is also noticed that the absorption peak expected in

vicinity of 3500cm^{-1} relevant to free hydroxyl group is absent. Absence indicates the involvement of $-\text{OH}$ group with an extensive H_2O interaction. Two bands at 2669 and 2561cm^{-1} are also observed which are assigned to the resonance between the fundamental mode of vibration and the in-plane bending of $-\text{OH}$ group. These observations are in concurrence with the reported [67] values. A strong absorption peak observed at 1697cm^{-1} is argued due to the $>\text{C}=\text{O}$ stretching of carboxylic acid. The peak observed at 1596cm^{-1} is assigned to the $>\text{CH}=\text{N}-$ of the Schiff's base intermediate, $(4)_{\text{MeO}}\text{BD}(3)_{\text{Am}}\text{BA}$.

In the IR spectra of 5OBA Strong absorption peaks (as a shoulder) at 3062cm^{-1} are assigned to $-\text{OH}$ group. Peaks observed at 2952cm^{-1} , 2869cm^{-1} are assigned to the C-H stretching modes of 5OBA. Absorption bands observed at 2661cm^{-1} and 2543cm^{-1} are assigned as resonant absorptions of fundamental vibrations and in-plane bending of the $-\text{OH}$ group. An absorption peak observed at 1919cm^{-1} with low intensity is assigned to the resonance mode of first and the second harmonics of the $-\text{OH}$ group. The fundamental mode of vibration of $-\text{OH}$ group is argued to merge with the C-H stretching. Absorption peak observed at 1676cm^{-1} due to carbonyl ($>\text{C}=\text{O}$) stretching mode (of 5OBA) concurs with the reports [68] and confirms the closed HB dimer configuration for 5OBA. The peaks observed at 1514 , 1577 and 1602cm^{-1} are attributed to the skeletal vibrations in the aromatic core.

A broad absorption peak in the range of $3055 - 2831\text{cm}^{-1}$ corresponding to the C-H stretching (in which the fundamental mode of vibration of $-\text{OH}$ is merged) is observed for FTIR spectrum of $(4)_{\text{MeO}}\text{BD}(3)_{\text{Am}}\text{BA}:5\text{OBA}$. The peaks at 2669cm^{-1} and 2553cm^{-1} correspond to the Fermi resonance between the fundamental mode and in-plane bending of $-\text{OH}$ moiety. The peak observed at 1897cm^{-1} is argued due to the resonance between first and second harmonics pertaining to $-\text{OH}$ moiety in the HBLC. A strong absorption peak observed at 1681cm^{-1} is assigned to the $>\text{C}=\text{O}$ stretching mode. An absorption peak observed at 1604cm^{-1} is argued to correspond to the Schiff's base. IR absorption peaks observed at 1512cm^{-1} are assigned to the $-\text{CH}=\text{CH}-$ stretching. The appearance of strong absorption observed at 1681cm^{-1} (pertaining to carbonyl $>\text{C}=\text{O}$ stretching of carboxylic acids) are found to accompany with a bathochromic shift of $\sim 5\text{cm}^{-1}$ (in comparison with that for 5OBA). They are also found to accompany with a hypsochromic shift of $\sim 15\text{cm}^{-1}$ with respect to $(4)_{\text{MeO}}\text{BD}(3)_{\text{Am}}\text{BA}$. Observed IR shifts infer that the carbonyl groups (of acids) participate in HB interaction. The absorption corresponding to $-\text{OH}$ group is

observed to manifest as a shoulder in all the three cases. But, it is observed to accompany with a shift to 3055cm^{-1} in HB complex, viz., from 3062cm^{-1} observed for respective carboxylic acids. Observed shift infers that the $-\text{OH}$ groups of both carboxylic acids participate in HB bond interaction. IR peak observed at 1681cm^{-1} is argued due to the carbonyl ($>\text{C}=\text{O}$) stretching mode and the closed (if not cyclic or nor homocynthon) configuration of constituent carboxylic acids.

An IR absorption at 941.24cm^{-1} is noticed in spectra of $(4)_{\text{MeO}}\text{BD}(3)_{\text{Am}}\text{BA}:5\text{OBA}$. This IR absorption is found to be comparable for the torsional γ -modes of $-\text{OH}$ moiety and due to Fermi resonance [68] in pure nOBAs with (945cm^{-1}) dimeric (and cyclic) HB interaction. It is also found to agree with the reported [65] torsional γ -modes of $-\text{OH}$ moiety pertaining to other organic compounds (948cm^{-1}) with HB interaction. A weak intensity IR absorption observed at 1913.25cm^{-1} is found to be comparable to that reported [65] for C-band relevant to $\nu(-\text{OH})$ mode in Pyridine+ CCl_4 system with HB. Hence, observed weak IR absorption is argued due to the C-band pertinent Fermi resonance of $-(\text{OH})$ stretching of $-\text{COOH}$ moiety (in the intermediate Schiff base meta-substituted acid) due to its participation in HB interaction.

Observed IR absorptions confirms [63] the presence of HB on the body of $(4)_{\text{MeO}}\text{BD}(3)_{\text{Am}}\text{BA}:\text{nOBA}$ type of LC complex. Since O-atom in the $-\text{COOH}$ of nOBA moieties interacts with H-atom of $-\text{COOH}$ of $(4)_{\text{MeO}}\text{BD}(3)_{\text{Am}}\text{BA}$ or vice versa, the HB is complementary type.

3c. Phase Characterization by POM Textures and Determination of Transition Temperatures (T_c)

The LC phases exhibited by present series of HBLC complexes are characterized by the POM textural observations [59,60] carried out during heating and cooling runs. The LC filled cells (or slides) are placed in the temperature controller kept on POM hot stage set for crossed polar configuration. The LC phases exhibited by $(4)_{\text{MeO}}\text{BD}(3)_{\text{Am}}\text{BA}:\text{nOBA}$ series of compounds along with the phase transition temperatures are presented in Table-2. The present series of HBLCs are found to exhibit SmA , SmB_{cry} , SmC , SmI , SmF and SmG phases.

SmA phase is observed to exhibit (Plate-1) focal conic fan, elongated (lathe-like) fan board (Plate-2) and spiked fan (Plate-3) textures. The spiked fan texture is found to be analogous to that reported [60] for TGBA version of SmA confined in homeotropic geometry. Although present series of HBLCs possess dominant

calamitic type of (Scheme-1) architectural features, the LC core looks like slightly bent structured with more mass on one side. Similarity between the textures exhibited by meta-extended core bearing HBLC and reported chiral LCs is argued due to the similarity of molecular architecture. It is noticed that the latter case [69,70] represents a one-sided mass loaded core with double and/or triple chiral centers. Meta-extension of rigid core is found to be akin to configuration of skewed mass in Cholesteryl Pelargonate. SmC phase is found to exhibit four brushed schlieren texture (Plate-4) as grown from the precursor SmA phase in heating run of (4)_{MeO}BD(3)_{Amn}BA:8OBA. SmC phase is found to exhibit black-on-white natural mosaic texture (Plate-5) also. SmB_{cry} is found to grow as colored mosaic (Plate-6) and glossy focal conic fan batonet textures (Plate-7). SmI is found to exhibit broken focal conic plume-like fan (Plate-8) texture when grown by cooling the SmB_{cry} in (4)_{MeO}BD(3)_{Amn}BA:8OBA. SmI is also found to exhibit colored threaded (Plate-9) texture in (4)_{MeO}BD(3)_{Amn}BA:12OBA. However, SmF is found to exhibit characteristic colored marble threaded texture (Plate-10) and checkered-board of elongated fan textures (Plate-11) in HBLC complex for n=9 and 12, respectively. In addition to the above textures, SmF is also found to exhibit a paramorphotic colored mosaic texture with undulated boundaries (Plate-12). Paramorphotic texture is found to be much akin to the undulated edge texture observed for n=11 in the cooling run. SmG exhibited characteristic colored mosaic (Plate-13) texture in the lower homologues of the present series of HBLCs.

LC phase variance is found to be large for n=8 and 12 compounds with ACIFG and AB_{cry}IFG phase sequences, respectively. It is observed that lower homologues (viz., for n≤6) and higher homologues (viz., for n=6 and 10 or 11) prevalently exhibit lower phase variance. It is also observed (Table-2) that LC clearing temperatures (T_{IC} , $T_{IB_{cry}}$, T_{IA}) and solid melting temperatures (T_{cry-LC}) exhibit O-E effect. However, O-E effect is rather rigorous at melting transitions to infer the dominant contributions [43-45] of axial polarizabilities. It is also noticed that the LC phase occurrence (in both of the heating and cooling scans) follows the standard hierarchy [59] and thermal order for growth of LC structural order.

It is noticed (Table-2) that although intermediate homologues do not exhibit 3D SmB_{cry} phase, lower homologues (for n=4 and 6) with short chain exhibit orthogonal (hexagonal) SmB_{cry} phase. Intermediate homologues (for n=7,8,9 and 10) do not exhibit 3D SmB_{cry} phase. However, higher homologues (for n=11 and



12) with large flexible chain exhibited this 3D $\text{SmB}_{\text{cryst}}$ phase with further increase of chain (n) length. Thus, $\text{SmB}_{\text{cryst}}$ phase appears to be re-entered with increasing flexibility in present HBLCs. Odd lower homologues, all intermediate homologues and higher homologues are found to exhibit enhanced tilted phase stability involving SmC , SmF , SmI and SmG phases. Compounds with $n=5,7,8,9,10,11$ and 12 exhibited dominant tilted phase stability. However, tilted LC phase abundance is rather predominant in intermediate homologues. Overall tilted phase abundance in HBLCs is observed to witness an enormous amount of increase in comparison with nOBAs. In comparison with [10] nOBA's, meta-extended core LCs (table-2) with O-atom as bridging atom are found to exhibit larger layered smectic polymorphism. Hence, the increased smectic phase abundance is argued due to predominant lateral stacking capability in meta-extended core LCs. It is interesting to notify that meta-extended rigid core, complementary hydrogen bonding and tunable flexibility (by varying length ' n ' of end chain) establish an effective set of molecular design parameters to promote tilted LC phase stability in HBLCs.

3d Differential Scanning Calorimetry

3d(i) Phase Transition Temperatures (T_c) and Enthalpy (ΔH) and LC Phase range

DSC thermogram recorded during heating and cooling scans for $(4)_{\text{MeO}}\text{BD}(3)_{\text{Am}}\text{BA:nOBAs}$ is presented (for $n=7$ as representative) in Figure-6. Data for the phase transition temperature (T_c) and the associated heats of transition (ΔH) observed during heating and cooling scans ($5^\circ\text{C}/\text{min}$) is presented in Table-2. Some of the peaks/valleys are observed to possess shoulders. In the case of DSC shoulders, the derivative curve is drawn to determine transition temperature T_c . Comparison of clearing transition temperatures and melting transition temperatures in nOBA's [10] with that in table-2 reveals that clearing temperatures witness a shift from a maximum value of 160°C (for $n = 4$ in nOBA's) to 121.8°C (for $n=11$ in meta-extended HBLCs). Nevertheless, the minimum of clearing temperature is also found to be shifted from 137°C (for $n = 12$ in nOBA's) to 91.8°C (for $n=10$ in meta-extended HBLCs). Analogously, comparison of maximum of melting transition temperatures in nOBA's and HBLC's also revealed a shift from 145°C (for $n = 3$ in nOBA's) to 112.2°C (for $n=4$ in meta-extended HBLCs). The minimum of melting temperature is also found to be shifted from 92°C (for $n = 7$ in nOBA's) to ambient temperatures (for $n=3$ in meta-extended HBLCs). An overview of the observed depression of clearing

and melting temperatures suggests that LCs with meta-extended core and complementary HB interaction results for the realization of LC phases structures towards ambient temperatures (rather than in their pristine LC components).

The enthalpy ΔH for DSC shoulders is argued to extend over two transitions. The ΔH for DSC shoulders is also presented in Table-2 with the extended dotted line over two transitions. The phase transition temperatures, viz., T_{I-A} , T_{I-C} , $T_{I-B_{cry}}$, T_{A-C} , T_{A-F} , T_{C-F} , T_{F-G} , $T_{B_{cry}-F}$, T_{C-SmI} , $T_{B_{cry}-SmI}$, T_{SmI-F} and $T_{G-Solid}$ determined by DSC are found to agree with the data of POM.

The observed finite ΔH across I-A, I-C, I- B_{cry} , C- B_{cry} , C-SmI, C-F, B_{cry} -SmI, B_{cry} -F, SmI-F, C-G, F-G, F-Sld and G-Sld transitions infer their first order nature. It may be noticed that A-C transition in present HBLCs is accompanied with no enthalpy or very small enthalpy to agree with the expected [1] to be of second ordered nature.

However, a small, but non-zero and finite (i.e., 0.39J/g across A-C transition for n=10) heat of transition is argued due to the small range of precursor SmA phase. As such, it is argued to be a case of fluctuation induced weak first order A-C transition. SmI-SmF transition involves a marginal change of tilt direction of pseudo hexagonal network (from apex to side). Its weak first order nature is argued due to the small thermal range of precursor SmI phase. However, slightly higher (or large) enthalpy is witnessed across SmI-SmF transition (in cooling scan) for n=8. Large enthalpy across this transition is attributed to the fluctuations.

3d(ii) Enantiotropic/Monotropic Phase Occurrence, LC Phase Variance and Chain length

Monotropic LC phase occurrence is observed for SmC and SmF phases for n=3 (in cooling run); SmG phase for n=6 (in heating run); SmF (in heating run) and SmG (in cooling run) for n=10; SmA for n=11 (in heating run) and SmI and SmF phases (in cooling run) for n=12. Relatively large Monotropic occurrence is found to occur in tilted smectic versions for even higher homologues. Higher homologues contain large flexible chain. Hence, orientational disorder caused by the large flexible component in HBLCs is argued to result for the prevalent monotropic occurrence. An overview of the data reveals that few number (~8) of monotropic phase occurrences appear out of a large number (~70) of total LC phase occurrences for meta-extended core constituted HBLCs, viz., in (4)_{MeO}BD(3)_{Am}BA:nOBAs. POM revealed that out of

ten HBLCs, six (viz., for $n = 3, 4, 5, 6, 10$ and 11) exhibited tri-variant LC phase abundance in cooling scan. Compounds with $n = 4, 5, 6$ and 11 are found to exhibit enantiotropic LC phases. Two HBLCs (for $n=7$ and 9) are found to exhibit enantiotropic tetra-variant LC phase abundance. Remaining two HBLCs (for $n=8$ and 12) exhibit penta-variant phase abundance in cooling scan. However, HBLC with $n=8$ exhibits enantiotropic phase occurrence. In HBLC with $n=12$, SmI and SmF phases appear as monotropic abundance in cooling scan. As Monotropic occurrence is very less, it may be concluded that enantiotropic LC phase occurrence is dominant in meta-extended HBLCs.



3e. Phase Diagram and Phase Stability

A phase diagram (Figure-7) is constructed with the help of data (Table-2 in cooling scan) to investigate the influence of flexible component (i.e., increasing chain length 'n') on the LC phase occurrence. A comparative study is made with the reported [10] data in nOBAs. As per the molecular structure (fig.-4) of $(4)_{MeO}BD(3)_{Am}BA:nOBAs$, flexible component is effectively tuned by increasing the end chain (n) length. Increasing the flexibility is effectively carried out by increasing the number of methylene units ($-CH_2$) at nOBA side of HBLC complex. Both of these series contain complementary type of HB interaction, while $(4)_{MeO}BD(3)_{Am}BA:nOBAs$ possess a meta-extended core. Such an analysis is anticipated to throw light on the possible impact of meta-extended core and increase in flexible (n) component for the abundance of LC polymorphism. Although both of them exhibited a decreasing trend of clearing temperatures with increasing flexibility, O-E effect at LC clearing interface (for where LC undergo clearing transition in to isotropic liquid) is observed to be more intense in meta-extended core HBLCs. Relatively decreasing trend of clearing transition infers that meta-extended core LCs are capable of bringing down the LC thermal stability towards ambient temperatures effectively. However, the O-E effect with increase of 'n' being relatively severe at solid melting interface (where solid melts in to LC phase), it reinstates that meta-extended core effectively brings down the LC phase temperatures to the room temperature range. It is noticed that tilted LC phase abundance (i.e., by origin of SmC phase) is initiated for $n>6$ in nOBA's. But, tilted LC phase abundance is observed for $n \geq 3$ in meta-extended core LCs. It is reckoned back that O-E effect is argued due to the alternating contributions [43-45] of axial polarizabilities, while odd homologues possess relatively more transverse dipole moment (μ_t) to pronounce tilted LC phase occurrence. O-E is expected to be

severe at solid melting transition involving LC phases with smaller inter-particle separation due to low temperature conditions. Hence, it is argued that meta-extended core LCs could promote μ_t more effectively to enhance the occurrence of tilted phases. Nematic phase is found to quench at $n = 14$ in nOBA's, while it is found absent even for $n = 3$ in the series of meta-extended core LCs. Nematic phase with orientational order is known to be stabilized by the longitudinal (μ_l) dipole moment. This observation clearly signifies that meta-extension of LC core exhibit a dominating suppressed trend of μ_l with a simultaneous increasing trend of μ_t which in turn enhance the occurrence of tilted phases.

Interesting and rare LC phase interface like SmI-SmF transition is witnessed for n equal to 8 and 12. Rare appearance of Iso-SmB_{cryst} LC phase transition is also witnessed for n equal to 4 and 11 in the meta-extended core constituted HBLCs.

From the phase diagram (Fig-7), Multi Critical Points (MCP) are noticed, where more than two phase structures with different structural order and symmetries converge. Symmetries with quasi-2D crystalline and pseudo-hexatic ordering in SmI, SmF and SmB_{hex} represent [2] exotic symmetries. Three phases are found to be involved with IAC (for $n=6$) and IAB_{cryst} (for $n=11$) MCPs devoid of exotic symmetries. Three phases are also found to be involved with CB_{cryst}F (for $n=3$), CIF (for $n=9$) and B_{cryst}IF (for $n=11$) MCP's involving exotic symmetries. Four different phases are found to be involved with IACB_{cryst} (for $n=4$) without exotic symmetries and ACB_{cryst}F (for $n=5$), CB_{cryst}IF (for $n=7$), CB_{cryst}FG (for $n=10$) MCP's with exotic symmetries.

The data for $[\Delta T]_{LC}$, $[\Delta T]_C$ and $[\Delta T]_{Tilt}$ estimated for resultant HBLCs are presented in Table-2. A histogram (Figure-8) is drawn for the LC phase abundance in (4)_{MeO}BD(3)_{Am}BA:nOBA's. However, for the sake of comparison, reported [9,32] data in nOBA's is also included in the figure.

A detailed analysis for the influence of flexible component (by increasing length (n) of (4)_{MeO}BD(3)_{Am}BA:nOBA) is also carried out (Figure-9) by plotting the relative LC phase stability, viz., through $[\Delta T]_{LC}$, $[\Delta T]_C$ and $[\Delta T]_{Tilt}$ with increasing length (n) of end chain. Estimation, presentation and analysis for trends in ΔT_{LC} , ΔT_{tilt} , ΔT_{ortho} and ΔT_C provide scope to study the influence of increasing flexibility and meta-extension of LC core. Further, ΔT in present HBLCs is also analyzed in the

wake of the data reported [9,40] for nOBA's. It is observed from the histogram, that pure nOBA's exhibited maximum LC phase stability for $n=7$ with a specific rigidity to flexibility ratio. With the increasing n , the ΔT_{LC} steeply increases to the maximum value, rather than its gradual trend of decreasing nature with further increase of flexibility for $n \geq 7$.

An integrated view of the Fig-8 and -9 reveals that occurrence of maximum $[\Delta T]_{LC}$ is achieved by the involvement of HB, which appears to be slightly pushed towards the higher flexible component (i.e. for $n=9$) in HBLCs. $[\Delta T]_{LC}$, $[\Delta T]_C$ and $[\Delta T]_{Tilt}$ are found to exhibit O-E effect. O-E effect is observed to be severe for present series of HBLCs regarding ΔT_{LC} and ΔT_{Tilt} . But, ΔT_{LC} for nOBA's and resultant HBLCs seems to follow an analogous trend with n when methylene ($-\text{CH}_2$) unit increment occurs for n equals to 3 to 4; 5 to 6; and 9 to 10 compounds. Commonality is that trends are similar when 'n' is increased to even number. However, a reversed trend for ΔT_{LC} is witnessed, when flexible component (n) is increased from even to odd i.e., from $n = 10$ to 11. ΔT_{LC} is found to exhibit intermediate magnitude of O-E effect in nOBA's. But, a large O-E effect is observed for HBLCs. $[\Delta T]_{Tilt}$ is found to be absent for $n \leq 6$ in nOBA's, while it is found to be finite for $n = 3$ onwards (up to 12) in meta-extended HBLCs of present interest. As both of the series contain complementary type of HB interaction, meta-extended core design feature in latter series is argued to result for increased tilt LC phase abundance.

$[\Delta T]_{Tilt}$ is found to exhibit an increasing trend for $n \geq 6$ for nOBAs. However, $[\Delta T]_{Tilt}$ exhibited a maximum range for $n=9$ in HBLCs despite the O-E effect. $[\Delta T]_{Tilt}$ is found to occupy higher values for $n=5, 7$ and 9 in HBLCs (except for $n=3$) being the odd numbered intermediate homologues. This observation of higher tilted LC phase stability agrees with the reports [28] of $[\Delta T]_{Tilt}$ for odd homologues. Odd homologue's contribution for tilted phases is argued due to outward projection of μ_t .

It is also argued that the existence of finite and/or enhanced LC phase stability in the HBLCs of pure nOBA's occurred due to meta-extended architecture

(Fig-4) of LC rigid core. Fig-4 reflects the supra-molecular aspects, viz., inclined HB interaction, meta-extended rigid core with underlying bent shape to molecular frame in addition to overall calamitic body/shape. In the present case of HBLCs, $[\Delta T]_{\text{Tilt}}$ is found to be higher (except for $n \geq 10$) for intermediate homologues than that reported [10] for nOBA's. Thus, meta-extended rigid core in HBLCs is inferred with larger phase stability for device savvy tilted smectic phases.

SmC phase stability $[\Delta T]_C$ is found to exhibit (fig-9) almost a monotonical increasing trend with 'n' (from $n \geq 6$ onwards) in pure nOBA's. But, $[\Delta T]_C$ in meta-extended core LCs is found to be accompanied with rigorous O-E effect with increasing 'n'. Hence, the increasing trend of $[\Delta T]_C$ behaviour with increase of flexibility seems to be suppressed in meta-extended core LCs. $[\Delta T]_C$ is also observed to bear higher value in higher (for $n \geq 9$) homologues of pure nOBA's. This observation infers the effective role played by orientational disorder in higher homologues, especially, which are not meta-extended core LCs. $[\Delta T]_C$ is also observed to attain higher value for even homologues of meta-extended core LCs. Appearance/existence of non-zero $[\Delta T]_C$ in HBLCs with $n=3$ and 6 presents a successful attempt by the involvement of meta extended HBLC architecture. Although nOBA's exhibited [10] almost monotonical increase of $[\Delta T]_C$ with increasing flexible (for $n > 6$) component, It is remarkable that the odd homologues of meta-extended core LCs exhibited lower values for $[\Delta T]_C$ in contrast to the general observation that odd homologues in any LC series exhibit enhanced tilted phase stability. This contrast behaviour for $[\Delta T]_C$ is argued due to the superposition of μ_t due to inclined configuration of HB interaction and meta-extended cores in out-of-phase configuration. $[\Delta T]_C$ is found (fig-8) to be almost quenched for $5 \leq n \leq 11$ in (except $n=3$) meta-extended core LCs. This observation infers that judicious flexible component is required to realize $[\Delta T]_C$ in meta-extended core LCs. $[\Delta T]_C$ seems to

be optimized in intermediate even numbered homologues for $n = 6, 8$ and 10 for meta-extended core LCs.

It is observed [10] that tilted phase or total LC phase range increases effectively with increasing chain length (n) in a series of LC compounds, especially, when chain length (n) crosses a threshold value. However, analogous increasing trends for $[\Delta T]_{LC}$ and $[\Delta T]_C$ with ' n ' are not observed for meta-extended HBLCs. As meta-extended HBLCs are visualized by a typical hybrid architecture with features (Fig-4) of calamitic and bent cores, trends of $[\Delta T]_{LC}$ and $[\Delta T]_C$ with ' n ' are argued to be dissimilar with regard to nOBA's.

3f. Integrated Heats of Transitions – Trends of Mesomorphism



Integrated enthalpy is estimated from the ΔH values of DSC data (Table-2) as $[\sum \Delta H]_{Heat}$ from heating scans and cooling scans $[\sum \Delta H]_{Cool}$; $\sum \Delta H$ are plotted (Figure-10) against the increased flexible (n) component in $(4)_{MeOBD}(3)_{Am}BA:nOBA$ HBLC complexes. $[\sum \Delta H]$ represents the heat energy transacted by the HBLC with the surroundings during its morphological changes in to the isotropic state. Thus, $[\sum \Delta H]_{Heat}$ reflects the heat energy required for the system to completely forego the orderly arrangement. But, $[\sum \Delta H]_{Cool}$ reveals the heat energy liberated from the HBLC, when isotropic liquid of HBLC is transformed back into 3D solid. $[\sum \Delta H]_{Heat}$ is found to occupy the negative ($-ve$) value as heat energy is supplied to the system and $[\sum \Delta H]_{Cool}$ occupy the positive ($+ve$) value as heat is evolved from the system during cooling scan. $[\sum \Delta H]$ exhibits O-E effect with increasing flexibility (n) component to infer [41,42,49] the relative susceptibility of axial polarizabilities.

It is noticed (fig-10) that $[\sum \Delta H]$ exhibits an overall increasing trend with increasing ' n ' in both of the heating and cooling scans for meta-extended core LCs. It is also observed that $[\sum \Delta H]_{Cool}$ is higher than $[\sum \Delta H]_{Heat}$ to infer higher energy transaction in restoring the order by cooling the sample. Differential heat energy consumption, i.e., $\delta(\sum H) = |\Delta H_H - \Delta H_C|$ is estimated for all HBLCs, during the heating followed by cooling scans. Trends of differential enthalpy with ' n ' is also presented in Fig-10 for meta-extended core LCs. The observed predominant occupancy in the negative Y-axis differential enthalpy $\delta[\sum \Delta H]$ is argued to vouch for the stability and growth of LC phases. More is the magnitude for differential enthalpy; more would be

the stability for expected LC phase appearance. Hence, optimized chain length (n) with largest differential enthalpy is argued as a characteristic value for the LC series under consideration. As such, the preferential order of stability with flexible component ' n ' is confirmed for $n = 3, 7, 9, 10$ and 12 in meta-extended LC cores. Hence, it is concluded that odd lower homologue for $n=3$, intermediate homologue for $n = 7$ and higher homologues for $n = 9, 10$ and 12 exhibit large device savvy LC phase stability due to the presence of meta-extended LC core.

In order to investigate the influence of meta-extended core on optimized growth (or stability) of LC phases, a comparative study of integrated and differential enthalpies is carried out (figures-11 and -12) for the meta-extended core LCs (table-2, which bear complementary [71,72] HB interaction with nOBA's and Schiff base containing [25] linear LC hydrogen bonded (4)PyBD(4^l)BrA-nOBA liquid crystal series. It is noticed that integrated enthalpies (fig-11) in both of the heating and cooling scans for complementary HB meta-extended or linear HB Schiff based LCs fall intermediate between the higher values of heating scan and lower values of cooling scan recorded for nOBA's. This observation speaks out the relatively comfortable growth of LC phase structures by exchange of lesser heat energy in meta-extended CL cores. Hence, involving either linear HB interaction or meta-extended core are argued to effectively stabilize the growth of LC phases. O-E effect for integrated enthalpy in the heating scan of nOBA's appears more rigorous than that observed for the heating scans of other two series of LCs. Apart from the O-E effect, the differential enthalpy (fig-12) is observed to accompany with relatively lesser values in nOBA's. Lesser values of $\delta(\Sigma H)$ for nOBA's infer involvement of lesser heat exchange in a cyclic scan of heating followed by cooling. Since, $\delta(\Sigma H)$ of meta-extended core LCs is more is least followed by linear HB Schiff based LCs, meta-extended core LC molecular design is argued to be a preferred direction of synthesis to realize LC phase structures of device savvy nature.

4 Conclusions

¹H-NMR and ¹³C-NMR spectral studies could be effective tools to confirm the presence of number and placement of H-atoms and C-atoms respectively, in the targeted LC molecule. IR-spectroscopic study can confirm the presence of hydrogen bonding interaction and its type in HBLC complexes. Preparation followed by phase characterization studies in (4)_{MeO}BD(3)_{Am}BA:nOBAs with meta-extended hybrid molecular architecture infer that presence of Schiff based moiety, meta-directed

1
2
3
4
5
6
7
8
9
10
11
12
13
14
15
16
17
18
19
20
21
22
23
24
25
26
27
28
29
30
31
32
33
34
35
36
37
38
39
40
41
42
43
44
45
46
47
48
49
50
51
52
53
54
55
56
57
58
59
60

extension of rigid core and complementary type of HB interaction prevails over the occurrence of tilted smectic polymorphism. Involvement of electro-negative O-atom (as bridging atom/group) promotes lateral stacking of molecules and enhanced smectic phase stability. Meta-extended rigid core in calamitic type of LCs witnesses quenching of Nematic phase due to the enhanced transverse dipole moment. Increase of flexible component in calamitic LC molecules induce orientational disorder to result for SmF and SmI like quasi-2D LC phases with exotic symmetries. Meta-extended rigid core results for ideal expectation of unique second order nature for A-C transition due to the effective contributions of transverse dipole moment. Meta extended rigid core of calamitic HBLC series with tunable (for n=3 to 12) flexible component could realize characteristic (i.e., for n=6) IAC **Multi Critical Point** (MCP) where exotic symmetries converge.

References

- [1] de Gennes PG. The Physics of Liquid Crystals. Ed: Marshall W, Wilkinson DH. Clarendon Press: Oxford, UK;1993.
- [2] Brock JD, Birgeneau RJ, Litster JD, Aharony A. Liquids, Crystals and Liquid Crystals. *PhysToday*. 1989;42:52-59.
- [3] Litster JD, Birgeneau RJ, Pershan PS. Phases and Phase Transitions. *Phys.Today*. 1982;35:26.
- [4] David J, Thouless F, Duncan M, Haldane J, Kosterlitz M. The Nobel Prize in Physics. 2016.
- [5] Gerhard P. Handbook of Liquid Crystals. Ch.III: Nematic Liquid Crystals. Ed: Demus D, Goodby J, Gray GW, Spiess HW, Vill V. Wiley VCH, Weinheim. 1998.
- [6] Clark NA, Lagerwall ST. Ferro-electric Liquid Crystals, Principles, Properties and Applications, Ed: Goodby JW, Blinc R, Clark NA, Lagerwall ST, Osipov MA, Pikin SA, Sakurai T, Yoshino K, Zeks B. Gordon & Breach Sci Publ. Philadelphia. 1991.
- [7] Priestley EB, Wojtowicz PJ, Sheng P. Introduction to Liquid Crystals. Plenum Press, New York and London, 2nd Printing. 1979.
- [8] Chandrasekhar S, Sadashiva BK, Suresh AK. Liquid Crystals of Disc like molecules. *Pramana*. 1977;7:471-480.
- [9] Paleos CM, Tsiourvas D. Thermotropic Liquid Crystals Formed by Intermolecular Hydrogen Bonding Interactions. *Angewandte Chemie International Edition in English*. 1995;34:1696-1711.
- [10] Sideratou Z, Tsiourvas D, Paleos CM, Skoulios A. Liquid crystalline behaviour of hydrogen bonded complexes of non-mesogenic Anil with p-n-alkoxybenzoic acids. *Liq Cryst*. 1997;22:51-60.
- [11] Kato T, Mizoshita N, Kanie K. Hydrogen Bonded Liquid Crystalline Materials: Supra molecular Polymeric assembly and the induction of Dynamic Function. *Macro Mol Rapid Commun*. 2001;22:797-814.
- [12] Kato T, Kato T, Fréchet JMJ, Uryu T, Kaneuchi F, Jin C, Fréchet JMJ. Hydrogen-bonded liquid crystals built from hydrogen-bonding donors and acceptors - Infrared study on the stability of the hydrogen bond between carboxylic acid and pyridyl moieties. *Liq Cryst*. 2006;33:1429-1437.
- [13] Reddy RA, Tschierske C. Bent-core liquid crystals: polar order, Superstructural chirality and spontaneous desymmetrisation in soft matter systems. *J Mater Chem*. 2006;16:907-961.

- [14] Tian YQ, Xu XH, Zhao YY, Tang XY, Li TJ, Huang XM. Synthesis of new phasmodic liquid crystals induced by intermolecular hydrogen bonding between pyridine moieties and carboxylic acids. *Mol Cryst Liq Cryst.*1998; 309:19-27.
- [15] Meier G, Sackmann E, Grabmaier JG. *Applications of Liquid Crystals.* Springer Verlag. New York. 1975.
- [16] Meyer RB. Ferroelectric Liquid Crystals; A Review. *Mol Cryst Liq Cryst.* 1977;40:33–48.
- [17] Demus D, Demus H,Zaschke H. *Flussgie Kristalle in Tabellen*, VEB DeutcherVerlag fur Grundestoffindustrie: Leipzig.1974.
- [18] Luckhurst GR, Gray GW. *The Molecular Physics of Liquid Crystals.* Academic Press, New York. 1979.Chpt.1:p.3-11
- [19] Pisipati VGKM. Polymesomorphism in N-(p-n-Alkoxybenzylidene)-p-n-Alkylanilines (nO.m) Compounds. *Z Naturforsch.* 2003;58a:661-663.
- [20] Weissflog W, Demus D. Compounds with lateral long-chain substituents-a new molecule structure concept for thermotropic liquid crystals. *Cryst Res Technol.*1983;18:K21-K24.
- [21] Weissflog W, Demus D. Thermotropic liquid crystalline compounds with lateral long-chain substituents (II):Synthesis and liquid crystalline properties of 1,4-Bis[4-substituted-benzoyloxy]-2-n-alkylbenzenes. *Cryst Res Technol.* 1984;19:55-64.
- [22] Coates D.The effect of lateral substitution on smectic C formation. *Liq Cryst.* 1987;2(4):423-428.
- [23] Bhagavath P, Mahabaleswara S. Bhatt SG, Potukuchi DM, ChalapathyPV, Srinivasulu M. Mesomorphic Thermal Stabilities in SupramolecularLiquid Crystals:Influence of the size and position of a substituent. *J Mol Liq.*2013; 186: 56-62.
- [24] Ashok Kumar AVN, Sridevi B, Srinivasulu M. Chalapathy PV,Potukuchi, DM. Inductive Effect for the phase stability in hydrogen bonded liquid crystal complexes, X-(p/m)BA:9OBAs. *Liq Cryst.* 2014; 41:184-196.
- [25] Krishna Murthy AVSN, ChalapathyPV,Srinivasulu M, Madhumohan MLN, Rao YV,Potukuchi DM. Influence of flexible chain, polar substitution and hydrogen bonding on phase stability in Schiff based (4)PyBD(4')BrA-nOBA series of liquid crystals. *Mol Cryst Liq Cryst.*2018;664:46-68.
- [26] Podoliak N, Novotná V, Kašpar M, Hamplová V, Pacherová O. Chiral smectogens with four-phenyl-ring molecular core, laterally substituted by iodine atom. *Liq Cryst.*2015; 42:404–411.

- [27] Kumar PA, Pisipati VGKM. Ambient Monocomponent Ferroelectric Liquid Crystals with a Wide Smectic-C* Range (< -20 to ≤ 65 °C). *Adv Mater.* 1998;12:1617-1619.
- [28] Subrao M, Potukuchi DM, Sharada RG, Bhagavath P, Bhat SG, Maddasani S. Novel biphenyl-substituted 1,2,4-oxadiazole ferroelectric liquid crystals: synthesis and characterization. *Beilstein J Org Chem.* 2015;11: 233–241.
- [29] Hall AW, Lacey D, Holmes D. Synthesis and Transition Temperatures of Some Branched Alkyloxycarbonylphenyl Esters of 3-(4'-n-Alkyl- and -alkoxy-biphenyl-4-yl)propanoic Acids and their Laterally Fluorinated Analogues. *Mol Cryst Liq Cryst.* 1994;250:333–346.
- [30] Mehmood H, Ahmad Z, Akhtar T, Siddiqi HM, Iqbal A, Hameed S, Tahir MN. Design, synthesis and liquid crystalline behavior of ethyl 4-((4-alkoxyphenyl)diazenyl)benzoates. *Mol Cryst Liq Cryst.* 2018;664:14–23.
- [31] Smith GW, Gardlund ZG. Liquid crystalline phases in a doubly homologous series of Benzylideneanilines - Textures and scanning Calorimetry. *J.Chem.Phys.* 1973;59(6):3214-3228.
- [32] Rananavare SB, Pisipati VGKM. An overview of liquid crystals based on Schiff base compounds. *Trans World Research Network.* 2011; ISBN: 978-81-7895-523-0:19-52.
- [33] Bhat SG, Srinivasulu M, Girish SR, Padmalatha PB, Mahabaleswara S, Potukuchi DM, Muniprasad M. Influence of Moieties and Chain length on the abundance of orthogonal and tilted phases of linear hydrogen bonded liquid crystals, Py16BA-nOBAs. *Mol Cryst Liq Cryst.* 2012;552:83-96.
- [34] Muniprasad M, Srinivasulu M, Chalapathy PV, Potukuchi DM. Induction of liquid crystalline phases and influence of chain length of Fatty acids in linear hydrogen bonded liquid crystal complexes. *Mol Cryst Liq Cryst.* 2012;557:102-117.
- [35] Muniprasad M, Srinivasulu M, Chalapathy PV, Potukuchi DM. Influence of chemical moieties and the flexible chain for the tilted smectic phases in linear hydrogen bonded liquid crystals with Schiff based Pyridene derivatives. *J Mol Struct.* 2012;1015:181-191.
- [36] Sridevi B, Chalapathy PV, Srinivasulu M, Pisipati VGKM, Potukuchi DM. Influence of hydrogen bonding on phase abundance in ferroelectric liquid crystals. *Liq Cryst.* 2004;31:303-310.
- [37] Suriyakala R, Pisipati VGKM, Narayanaswamy G, Potukuchi DM. Alternating Intermolecular hydrogen bonding in linear liquid crystalline complexes. *Mol Cryst Liq Cryst.* 2006;457:181-189.
- [38] Vijay Kumar VN, Madhumohan MLN. A Study of Light Modulation and Field Induced Transition (FiT). *Mol Cryst Liq Cryst.* 2010;517:113-126.

- [39] Muniprasad M, Madhumohan MLN, Chalapathi PV, Ashokkumar AVN, Potukuchi DM. Influence of spacer and flexible chain on polymorphism in complementary hydrogen bonded liquid crystal dimers, SA:nOBAs. *J Mol Liq*. 2015; 207:294–308.
- [40] Ashokkumar AVN, Chalapathi PV, Srinivasulu M, Muniprasad M, Potukuchi DM. Influence of spacer moiety and length of end chain for the phase stability in complementary, double hydrogen bonded liquid crystals, MA:nOBAs. *J Mol Str*. 2015; 1079:94–110.
- [41] Vijayakumar VN, Murugadass K, Mohan MLNM. A Study of Reentrant Smectic Ordering in Hydrogen Bonded Ferroelectric Dodecyloxy Benzoic Acid and Tartaric Acid Liquid Crystal. *Mol Cryst Liq Cryst*. 2010; 517:43–62.
- [42] Subhapiya P, Vijayakumar VN, Mohan MLNM, Vijayanand PS. Study and Characterization of Double Hydrogen-Bonded Liquid Crystals Comprising p-n Alkoxy Benzoic Acids with Azelaic and DodecaneDicarboxylic Acids. *Mol Cryst Liq Cryst*. 2011; 537:36–50.
- [43] Marčelja S. Chain ordering in liquid crystals.I. Even-odd effect. *J Chem Phys*. 1974; 60:3599–3604.
- [44] Blumstein A, Thomas O. Odd-even effect in thermotropic liquid crystalline 4,4'-dihydroxy-2,2'-dimethylazoxybenzene-alkanedioic acid polymer. *Macro mol*. 1982; 15:1264–1267.
- [45] Itahara T, Tamura H. Odd–Even Effect in Liquid Crystal Tetramers. *Mol. Cryst. Liq Cryst*. 2009; 501:94–103.
- [46] Demus D. Molecular structure of Nematic liquid crystals. *J Chem*. 2010; 26:6-15.
- [47] de Vries A. *Liquid Crystals and Ordered Fluids*. Ed.Griffin C, Julian F and Johnson F. Plenum press, Newyork. 1982; 4:137-153.
- [48] Padmaja S, NancharaRao MRK, Datta Prasad, PV, Pisipati VGKM. Studies of Orientational Disorder at Isotropic to Smectic-F interface. *Z Naturforsch*. 60a:296-300.
- [49] Guilbert AAY, Frost JM, Agostinelli T, Pires E, Lilliu S, Macdonald JE, Nelson J. Influence of Bridging Atom and Side Chains on the Structure and Crystallinity of Cyclopentadithiophene–Benzothiadiazole Polymers. *Chemistry of Materials*. 2014; 26(2):1226–1233.
- [50] Subrahmanyam SV, Chalapathi PV, Mahabaleswara S, Srinivasulu M, Potukuchi DM. Ferroelectric phases in non-symmetric achiral bent liquid crystals towards ambient temperatures: a novel series with oxadiazol as central moiety. *Liq Cryst*. 2014; 41:1130–1151.

- [51] Niori T, Sekine T, Watanabe J, Furukawa T, Takezoe H. Distinct ferroelectric smectic liquid crystals consisting of banana shaped achiral molecules. *J Mater Chem*. 1996;6:1231-1233.
- [52] Shen D, Diele S, Pelzl G, Wirth I, Tschierske C. Designing banana-shaped liquid crystals without Schiff's base units: m-terphenyls, 2,6-diphenylpyridines and V-shaped tolane derivatives. *J Mater Chem*. 1999;9:661-672.
- [53] Cano M, Sánchez FA, Serrano JL, Gimeno N, Ros MB. Supramolecular Architectures from Bent-Core Dendritic Molecules. *Ang Chem Int Ed*. 2014;53,13449–13453.
- [54] Gimeno N, Ros MB, Serrano JL, De la Fuente MR. Noncovalent Interactions as a Tool To Design New Bent-Core Liquid-Crystal Materials. *Chemistry of Materials*, 2008;20,1262–1271.
- [55] Paterson DA, Crawford CA, Pocięcha D, Walker R, Storey JMD, Gorecka E, Imrie CT. The role of a terminal chain in promoting the twist-bend nematic phase: the synthesis and characterisation of the 1-(4-cyanobiphenyl-4'-yl)-6-(4-alkyloxyanilinebenzylidene-4'-oxy)hexanes. *Liq Cryst*. 2018;45(1), 1–11.
- [56] Abberley JP, Jansze SM, Walker R, Paterson DA, Henderson PA, Marcelis A TM, Imrie CT. Structure–property relationships in twist-bend nematogens: the influence of terminal groups. *Liq Cryst*. 2017;1–16.
- [57] Pisula W, Müllen K. Discotic Liquid Crystals as Organic Semiconductors. *Hand book of Liquid Crystals*. 2014;1–47.
- [58] Balagurusamy VSK, Prasad SK, Chandrasekhar S, Kumar S, Manickam M, Yelamagad CV. Quasi-one dimensional electrical conductivity and Thermo electric power studies on a discotic liquid crystal. *Pramana*. 1999;53:3-11.
- [59] Gray GW, Goodby JW. *Smectic liquid crystals-textures and structures*. London: Leonard Hill. 1984.
- [60] Dierking I. *Textures of liquid crystals*. Weinheim: Wiley-VCH Verlag, GmbH, KGaA; p.156 and 183, 2003.
- [61] Silverstein RM, Webster FX. *Spectroscopic Identification of Organic Compounds*. 6th Ed, John Wiley and Sons Inc. New York. 2004.
- [62] William K. *Organic Spectroscopy*, Replika Press, India. 2008.
- [63] Nakamoto K. *Infra-Red and Raman Spectra of Inorganic and Coordination Compounds*, 4th Ed. Inter Science. New York. 1978.
- [64] Bratoz S, Hazdi D, Sheppard N. The infra-red absorption bands associated with the COOH and COOD groups in dimeric carboxylic acid—II: Region from 3700 to 1500 cm⁻¹. *Spectrochim. Acta*. 1956;8:249-261.

- [65] Odinokov SE, Iogansen AV. Torsional γ -(OH) vibrations, Fermi resonance 2γ (OH) and ν (OH) and isotopic effects in i.r. Spectra of H-complexes of Carboxylic acids with strong Bases. *Spectrochim Acta Part A-Mol Spectr.* 1972; A28:2343-2350.
- [66] Odinokov SE, Mashkovsky AA, Glazunov VP, Iogansen AV, Rassadin BV. Spectral Manifestations of Intermolecular and Interionic Hydrogen-Bonding in Adducts of various Acids with Pyridine. *Spectrochim Acta Part A-Mol and Biomol Spectr.* 1976;32:1355-1363.
- [67] Martinez-Felipe A, Cook AG, Abberley JP, Walker R, Storey JMD, Imrie CT. An FT-IR spectroscopic study of the role of hydrogen bonding in the formation of liquid crystallinity for mixtures containing bipyridines and 4-pentyloxybenzoic acid. *Rsc. Advances.* 2016;108164-108179.
- [68] Abdy MJ, Murdoch A, Martinez-Felipe A. New insights into the role of hydrogen bonding on the liquid crystal behaviour of 4-alkoxybenzoic acids: a detailed IR spectroscopy study. *Liq. Cryst.*, doi:10.1080/02678292.2016.1212119.
- [69] Kaspar M, Hamplova V, Novotna V, Glogorova M, Pociacha D, Vanek P. New series of ferroelectric liquid crystals with two or three chiral centres exhibiting antiferroelectric and hexatic phases. *Liq Cryst.* 2001;28:1203-1209.
- [70] Yoshizawa A, Yokoyama A, Nishiyama I. The effects of a second branched alkylchain and double chiral centres on the phase transition and spontaneous polarization of a chiral smectic liquid crystal. *Liq Cryst.* 1992;11:235-249.
- [71] Herbert AJ. Transition temperatures and transition energies of p-n-alkoxy benzoic acids, from n-propyl to n-octadecyl. 1967;555-560.
- [72] Kumar PA, Srinivasulu M, Pisipati VGKM. Induced smectic G phase through intermolecular hydrogen binding. *Liq Cryst.* 1999;26:1339-1343.

CAPTIONS

Scheme-1: Synthetic route for the preparation of $(4)_{\text{MeO}}\text{BD}(3)_{\text{Am}}\text{BA:nOBA}$.

FIGURES

Figure-1: Diversity of liquid crystal molecular architecture.

Figure-2 : ^1H NMR spectra of $(4)_{\text{MeO}}\text{BD}(3)_{\text{Amn}}\text{BA:5OBA}$.

Figure-3 : ^{13}C NMR spectra of $(4)_{\text{MeO}}\text{BD}(3)_{\text{Amn}}\text{BA:5OBA}$

Figure-4 : Hybrid molecular structure for $(4)_{\text{MeO}}\text{BD}(3)_{\text{Am}}\text{BA:nOBA}$'s with calamitic and bent features.

Figure-5: FTIR spectra of $(4)_{\text{MeO}}\text{BD}(3)_{\text{Am}}\text{BA:5OBA}$ and its pristine compounds.

Figure-6: DSC thermogram of $(4)_{\text{MeO}}\text{BD}(3)_{\text{Amn}}\text{BA:7OBA}$.

Figure-7: Phase diagram for $(4)_{\text{MeO}}\text{BD}(3)_{\text{Amn}}\text{BA:nOBAs}$

Figure-8: LC Phase stability for $(4)_{\text{MeO}}\text{BD}(3)_{\text{Am}}\text{BA:nOBAs}$.

Figure-9: Trends of Phase stability ΔT with flexible component n .

Figure-10: Integrated heats ($\sum\Delta H_{\text{H}}$ and $\sum\Delta H_{\text{C}}$) and Differential heat $\delta\sum\Delta H$ for $(4)_{\text{MeO}}\text{BD}(3)_{\text{Am}}\text{BA:nOBAs}$.

Figure-11: Comparison of integrated enthalpy of $(4)_{\text{MeO}}\text{BD}(3)_{\text{Am}}\text{BA:nOBA}$'s with Schiff based $(4)\text{PyBD}(4^{\text{I}})\text{BrA-nOBA}$'s and nOBA 's.

Figure-12: Comparison of differential enthalpy of $(4)_{\text{MeO}}\text{BD}(3)_{\text{Am}}\text{BA:nOBA}$'s with Schiff based $(4)\text{PyBD}(4^{\text{I}})\text{BrA-nOBA}$'s and nOBA 's.

TABLES

Table-1: Data of IR absorption for $(4)_{\text{MeO}}\text{BD}(3)_{\text{Am}}\text{BA:nOBAs}$.

Table-2: Data of LC phases, T_{C} and ΔH from POM and DSC for $(4)_{\text{MeO}}\text{BD}(3)_{\text{Am}}\text{BA:nOBAs}$.

PLATES

Plate-1: SmA focal conic fan texture of $(4)_{\text{MeO}}\text{BD}(3)_{\text{Amn}}\text{BA:11OBA}$ at 119.3°C (heating).

Plate-2: SmA elongated lathe-like extended-board texture of $(4)_{\text{MeO}}\text{BD}(3)_{\text{Amn}}\text{BA:7OBA}$ at 115.6°C (cooling).

Plate-3: SmA spiked fan texture of $(4)_{\text{MeO}}\text{BD}(3)_{\text{Amn}}\text{BA:10OBA}$ at 90.9°C (heating).

Plate-4: SmC four brushed schleiren texture of $(4)_{\text{MeO}}\text{BD}(3)_{\text{Amn}}\text{BA:8OBA}$ at 109.8°C (heating).

1
2
3
4
5
6
7
8
9
10
11
12
13
14
15
16
17
18
19
20
21
22
23
24
25
26
27
28
29
30
31
32
33
34
35
36
37
38
39
40
41
42
43
44
45
46
47
48
49
50
51
52
53
54
55
56
57
58
59
60

- Plate-5:** SmC black-on-white natural mosaic texture of (4)_{MeO}BD(3)_{Amn}BA:6OBA at 107.2°C(heating).
- Plate-6:** SmB_{cry} colored mosaic texture of (4)_{MeO}BD(3)_{Amn}BA:11OBA at 105.7°C (heating).
- Plate-7:** SmB_{cry} glossy focal conic fan batonnet texture of (4)_{MeO}BD(3)_{Amn}BA:6OBA at 90.2°C (cooling).
- Plate-8:** SmI broken focal conic plume texture of (4)_{MeO}BD(3)_{Amn}BA:8OBA at 95.8°C(cooling).
- Plate-9:** SmI colored threaded texture of (4)_{MeO}BD(3)_{Amn}BA:12OBA at 102.7°C (cooling).
- Plate-10:** SmF colored marble threaded texture of (4)_{MeO}BD(3)_{Amn}BA:9OBA at 98.3°C(heating).
- Plate-11:** SmF checkered-board texture with elongated fans of (4)_{MeO}BD(3)_{Amn}BA:12OBA at 87.8°C(cooling).
- Plate-12:** SmF paramorphotic coloured mosaic texture with undulated boundaries of (4)_{MeO}BD(3)_{Amn}BA:11OBA at 103.3°C(cooling).
- Plate-13:** SmG coloured mosaic texture of (4)_{MeO}BD(3)_{Amn}BA:8OBA at 91.5°C(cooling).

Appendix-A

NMR spectra is analyzed [61,62] to determine the presence of H-atoms on the body of HBLC. Data for observed chemical shifts (δ_H) for all members of (4)_{MeO}BD(3)_{Amn}BA:nOBA series of HBLCs (for n=3,4,5,6,7,8,9,10,11 and 12) is:

¹H NMR Study

(4)_{MeO}BD(3)_{Amn}BA:3OBA is observed with chemical shift (δ_H); 1.05 (3H, t, J = 7.5 Hz, -CH₃), 1.78-1.90 (2H, m, -OCH₂CH₂CH₂-), 3.88 (3H, s, -O-CH₃), 3.97-4.01 (2H, t, J = 6.6 Hz, -OCH₂-CH₂-), 6.92-8.07 (12H, m, Ar-H), 8.43 (1H, s, -CH=N), 9.89 (1H, s, -COOH).

(4)_{MeO}BD(3)_{Amn}BA:4OBA is observed with chemical shift (δ_H); 0.99 (3H, t, J = 6.9 Hz, -CH₃), 1.44-1.57 (2H, m, -[CH₂]₁-), 1.75-1.82 (2H, m, -OCH₂CH₂CH₂-), 3.88 (3H, s, -O-CH₃), 4.01-4.05 (2H, t, J = 6.6 Hz, -OCH₂-CH₂-), 6.92-8.07 (12H, m, Ar-H), 8.43 (1H, s, -CH=N), 9.89 (1H, s, -COOH).

(4)_{MeO}BD(3)_{Amn}BA:5OBA is observed with chemical shift (δ_H); 0.91 (3H, t, J = 6.9 Hz, -CH₃), 1.33-1.50 (4H, m, -[CH₂]₂-), 1.77-1.86 (2H, m, -OCH₂CH₂CH₂-), 3.88 (3H, s, -O-CH₃), 4.00-4.04 (2H, t, J = 6.6 Hz, -OCH₂-CH₂-), 6.92-8.07 (12H, m, Ar-H), 8.43 (1H, s, -CH=N), 9.89 (1H, s, -COOH).

(4)_{MeO}BD(3)_{Amn}BA:6OBA is observed with chemical shift (δ_H); 0.91 (3H, t, J = 6.9 Hz, -CH₃), 1.32-1.49 (6H, m, -[CH₂]₃-), 1.76-1.85 (2H, m, -OCH₂CH₂CH₂-), 3.88 (3H, s, -O-CH₃), 4.00-4.04 (2H, t, J = 6.6 Hz, -OCH₂-CH₂-), 6.92-8.07 (12H, m, Ar-H), 8.43 (1H, s, -CH=N), 9.89 (1H, s, -COOH).

(4)_{MeO}BD(3)_{Amn}BA:7OBA is observed with chemical shift (δ_H); 0.90 (3H, t, J = 6.9 Hz, -CH₃), 1.31-1.49 (8H, m, -[CH₂]₄-), 1.76-1.85 (2H, m, -OCH₂CH₂CH₂-), 3.89 (3H, s, -O-CH₃), 4.00-4.04 (2H, t, J = 6.6 Hz, -OCH₂-CH₂-), 6.92-8.07 (12H, m, Ar-H), 8.43 (1H, s, -CH=N), 9.89 (1H, s, -COOH).

(4)_{MeO}BD(3)_{Amn}BA:8OBA is observed with chemical shift (δ_H); 0.89 (3H, t, J = 6.9 Hz, -CH₃), 1.29-1.47 (10H, m, -[CH₂]₅-), 1.76-1.85 (2H, m, -OCH₂CH₂CH₂-), 3.89 (3H, s, -O-CH₃), 4.00-4.04 (2H, t, J = 6.6 Hz, -OCH₂-CH₂-), 6.92-8.07 (12H, m, Ar-H), 8.43 (1H, s, -CH=N), 9.89 (1H, s, -COOH).

(4)_{MeO}BD(3)_{Amn}BA:9OBA is observed with chemical shift (δ_H); 0.88 (3H, t, J = 6.9 Hz, -CH₃), 1.28-1.48 (12H, m, -[CH₂]₆-), 1.76-1.83 (2H, m, -OCH₂CH₂CH₂-), 3.89 (3H, s, -O-CH₃), 4.00-4.04 (2H, t, J = 6.6 Hz, -OCH₂-CH₂-), 6.92-8.07 (12H, m, Ar-H), 8.43 (1H, s, -CH=N), 9.89 (1H, s, -COOH).

(4)_{MeO}BD(3)_{Amn}BA:10OBA is observed with chemical shift (δ_H); 0.88 (3H, t, $J = 6.9\text{Hz}$, $-\text{CH}_3$), 1.28-1.46 (14H, m, $-\text{[CH}_2\text{]}_{7-}$), 1.76-1.85 (2H, m, $-\text{OCH}_2\text{CH}_2\text{CH}_2-$), 3.88 (3H, s, $-\text{O}-\text{CH}_3$), 3.99-4.04 (2H, t, $J = 6.6\text{ Hz}$, $-\text{OCH}_2-\text{CH}_2-$), 6.91-8.07 (12H, m, Ar-H), 8.43 (1H, s, $-\text{CH}=\text{N}$), 9.89 (1H, s, $-\text{COOH}$).

(4)_{MeO}BD(3)_{Amn}BA:11OBA is observed with chemical shift (δ_H); 0.88 (3H, t, $J = 6.9\text{Hz}$, $-\text{CH}_3$), 1.27-1.46 (16H, m, $-\text{[CH}_2\text{]}_{8-}$), 1.76-1.85 (2H, m, $-\text{OCH}_2\text{CH}_2\text{CH}_2-$), 3.89 (3H, s, $-\text{O}-\text{CH}_3$), 4.00-4.02 (2H, t, $J = 6.6\text{ Hz}$, $-\text{OCH}_2-\text{CH}_2-$), 6.91-8.07 (12H, m, Ar-H), 8.43 (1H, s, $-\text{CH}=\text{N}$), 9.90 (1H, s, $-\text{COOH}$).

(4)_{MeO}BD(3)_{Amn}BA:12OBA is observed with chemical shift (δ_H); 0.88(3H, t, $J=6.9\text{Hz}$, $-\text{CH}_3$), 1.27-1.46 (18H, m, $-\text{[CH}_2\text{]}_{9-}$), 1.76-1.85 (2H, m, $-\text{OCH}_2\text{CH}_2\text{CH}_2-$), 3.88 (3H, s, $-\text{O}-\text{CH}_3$), 3.99-4.02(2H, t, $J=6.6\text{ Hz}$, $-\text{O}-\text{CH}_2-\text{CH}_2-$), 6.91-8.07 (12H, m, Ar-H), 8.43 (1H, s, $-\text{CH}=\text{N}$), 9.89(1H, s, $-\text{COOH}$).

¹H NMR study for (4)_{MeO}BD(3)_{Am}BA:5OBA HBLC (Fig-2) as Representative:

As per the molecular formula for $n=5$ in Scheme-1, the number of H-atoms expected to be on the molecular body of (4)_{MeO}BD(3)_{Am}BA:5OBA is 29.

Salient features of the observed ¹H NMR spectra are;

- A triplet at $\delta 0.91\text{ppm}$ infers the presence of 3-H atoms relevant to end methyl group of 5OBA moiety.
- A multiplet at $\delta 1.33\text{--}1.86\text{ppm}$ infers the presence of 6-H atoms relevant to three methylene ($-\text{CH}_2-$) units of 5OBA.
- A singlet in the range of $\delta 3.88\text{ppm}$ infers the presence of 3-H atoms pertaining to methoxy ($-\text{OCH}_3$) group connected to Schiff base intermediate.
- A triplet at $\delta 4.00\text{--}4.04\text{ppm}$ infers the presence of 2-H atoms pertaining $-\text{OCH}_2$ group of 5OBA.
- A multiplet in the range of at $\delta 6.92\text{--}8.07\text{ppm}$ infers the presence of 12-H atoms corresponding to three aromatic rings (Ar-H) of HBLC complex.
- A singlet at $\delta 8.43\text{ppm}$ infers the presence of 1-H atom pertaining to the Schiff base $\text{CH}=\text{N}$ moiety.
- A signal (by integrated envelope) in the range of $\delta 10.2\text{--}11.6\text{ppm}$ infers the presence of 2-H atoms pertaining to the two acid ($-\text{COOH}$) moieties that participate in HB.

An overview of ¹H NMR spectra (points a-g) infers the presence of TWENTY NINE H-atoms on the molecular body of the HBLC. Since observed number of H-atoms is

found to agree with expected number of H-atoms, the targeted synthesis is argued to be successful. The HBLC product is argued to be pure to spectroscopic level.

It is also noticed (Fig-2) that chemical shift relevant to the H-atom pertaining to hydroxyl (-OH) moieties (i.e., Schiff based intermediate and nOBA) of acid groups (-COOH) is found ($\delta \sim 10-12$) to vouch [61,62] for the de-shielding effect due to their vicinity to the HB interaction.

Appendix-B

¹³C NMR Study

The presence of C-atoms on the body of HBLC complexes is estimated [61,62] from the ¹³C-NMR spectra. Data for chemical shift are presented here for all the ten resulting HBLCs (n=3-12).

(4)_{MeO}BD(3)_{Amn}BA:3OBA

δ_C : 10.42, 22.41, 55.42, 55.55, 69.72, 114.18, 114.26, 116.27, 120.27, 120.45, 121.36, 121.86, 127.00, 127.20, 128.87, 129.23, 129.35, 130.46, 130.77, 132.00, 132.33, 152.51, 160.86, 162.55, 163.70, 172.04, 190.90.

(4)_{MeO}BD(3)_{Amn}BA:4OBA

δ_C : 13.78, 19.16, 31.10, 55.42, 55.55, 67.95, 114.17, 114.26, 116.27, 120.27, 120.45, 121.34, 121.86, 127.01, 127.20, 128.86, 129.23, 129.34, 130.45, 130.77, 132.00, 132.32, 152.51, 160.86, 162.54, 163.71, 172.05, 190.89.

(4)_{MeO}BD(3)_{Amn}BA:5OBA

δ_C : 13.97, 22.40, 28.17, 28.76, 55.42, 55.55, 68.27, 114.19, 114.27, 116.28, 120.28, 120.46, 121.35, 121.87, 127.01, 127.21, 128.88, 129.24, 129.35, 130.46, 130.78, 132.01, 132.33, 146.42, 152.52, 160.86, 162.56, 163.71, 172.05, 172.36, 190.89.

(4)_{MeO}BD(3)_{Amn}BA:6OBA

δ_C : 13.98, 22.54, 25.62, 29.02, 31.50, 55.40, 55.53, 68.27, 114.17, 114.25, 116.27, 120.27, 120.45, 121.34, 121.86, 127.00, 127.20, 128.86, 129.22, 129.33, 130.46, 130.77, 132.00, 132.32, 146.40, 152.49, 160.86, 162.54, 163.70, 172.08, 172.39, 190.89.

(4)_{MeO}BD(3)_{Amn}BA:7OBA

δ_C : 14.05, 22.58, 25.92, 29.00, 29.07, 31.73, 55.42, 55.55, 68.28, 114.19, 114.26, 116.27, 120.27, 120.46, 121.35, 121.87, 127.01, 127.20, 128.88, 129.24, 129.35, 130.37, 130.46, 130.78, 132.01, 132.33, 146.42, 152.52, 160.86, 162.55, 163.71, 172.05, 190.89.

(4)_{MeO}BD(3)_{Amn}BA:8OBA

δ_C : 14.08, 22.64, 25.98, 29.09, 29.20, 29.31, 31.79, 55.45, 55.58, 69.31, 114.21, 114.28, 116.24, 120.23, 120.44, 121.33, 121.87, 127.00, 127.19, 128.93, 129.25, 129.38, 130.34, 130.43, 130.77, 132.01, 132.34, 146.47, 152.59, 160.82, 162.56, 163.72, 171.78, 172.07, 190.86.

(4)_{MeO}BD(3)_{Amn}BA:9OBA

δ_C : 14.05, 22.62, 25.93, 29.05, 29.20, 29.32, 29.47, 31.83, 55.40, 55.53, 68.26, 114.17, 114.24, 116.25, 120.24, 120.44, 121.33, 121.85, 126.99, 127.18, 128.87, 129.21, 129.33, 130.44, 130.75, 131.99, 132.31, 146.40, 152.50, 160.83, 162.53, 163.69, 164.61, 172.02, 172.33, 190.86.

(4)_{MeO}BD(3)_{Amn}BA:10OBA

δ_C : 14.07, 22.64, 25.94, 29.06, 29.28, 29.32, 29.51, 31.86, 55.40, 55.53, 68.27, 114.17, 114.24, 116.27, 120.23, 120.44, 121.35, 121.84, 126.98, 127.19, 128.87, 129.21, 129.32, 130.50, 130.76, 131.99, 132.31, 146.39, 152.49, 160.82, 162.53, 163.69, 172.02, 172.34, 190.86.

(4)_{MeO}BD(3)_{Amn}BA:11OBA

δ_C : 14.08, 22.65, 25.94, 29.06, 29.31, 29.56, 31.88, 55.42, 55.55, 68.28, 114.18, 114.25, 116.24, 120.24, 120.44, 121.31, 121.86, 127.00, 127.19, 128.89, 129.23, 129.35, 130.42, 130.76, 131.99, 132.33, 146.42, 152.54, 160.83, 162.54, 163.71, 171.95, 172.26, 190.86.

(4)_{MeO}BD(3)_{Amn}BA:12OBA

δ_C : 14.07, 22.65, 25.94, 29.05, 29.31, 29.54, 29.60, 31.88, 55.40, 55.53, 68.26, 114.16, 114.24, 116.25, 120.21, 120.43, 121.37, 121.83, 126.95, 127.18, 128.88, 129.20, 129.32, 130.41, 130.54, 130.75, 131.99, 132.30, 146.40, 152.50, 160.80, 162.52, 163.67, 171.96, 172.28, 190.86.

The number of C-atoms in of (4)_{MeO}BD(3)_{Am}BA:nOBA (for n=3 to 12) is estimated from the observed ^{13}C NMR chemical shifts (δ_C). ^{13}C -NMR spectra for (4)_{MeO}BD(3)_{Amn}BA:5OBA is presented in [Figure-3](#) (representative). As per the proposed ([Scheme-1](#)) molecular formula, (4)_{MeO}BD(3)_{Amn}BA:5OBA is expected to possess TWENTY SEVEN C-atoms on its molecular body.

Salient features of the ^{13}C NMR spectrum are;

- i) A peak at δ 3.97 ppm infers the presence one C-atom of end methyl carbon of 5OBA.

ii) Peaks in the range of $\delta 22.4$ – 28.8 ppm infer the presence of three C-atoms relevant to the three methylene ($-\text{CH}_2-$) groups of 5OBA.

iii) Peak at $\delta 55.9$ ppm infers the presence of one C-atom corresponding to the methoxy ($-\text{OCH}_3$) group of schiff base moiety connected at para position of aromatic ring .

iv) Peak at $\delta 68.27$ ppm infers the presence of one C-atom adjacent to O-atom of 5OBA moiety.

v) Peaks in the range of $\delta 114.19$ - 152.52 ppm infer the presence of eighteen C-atoms of three aromatic rings in HBLC.

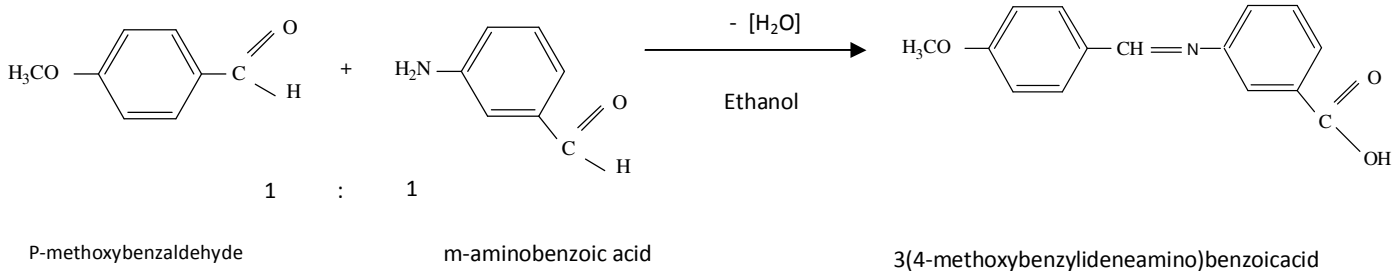
vi) Peak at $\delta 160.86$ ppm infers the presence of one carbon atom in the Schiff base ($\text{CH}=\text{N}-$) moiety.

vii) Peaks in range of $\delta 172.05$ - 172.36 ppm infer the presence of two carbon atoms pertaining to the two acid ($-\text{COOH}$) moieties.

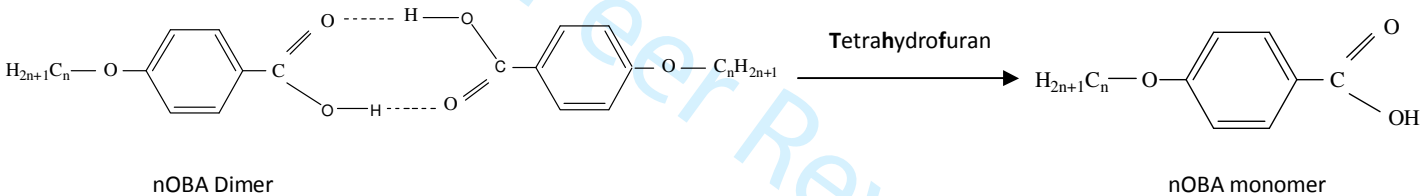
An overview of the NMR (from i to vii) spectrum infers that TWENTY SEVEN C-atoms are present on the body of $(4)_{\text{MeO}}\text{BD}(3)_{\text{Amn}}\text{BA:5OBA}$. Since, observed number of C-atoms agrees with the expected, the targeted synthesis of HBLC complex is argued to be successful. Further, HBLC is also argued to be pure to spectroscopic level.

It is also noticed (Fig-3) that the NMR signals (for C-atom) pertaining to the para-positioned (to nOBA) and meta positioned (Schiff based intermediate) acid ($-\text{COOH}$) moieties are found to be witnessed ($\delta 10.2$ – 11.6) to imply [61,62] a shift due to their vicinity to HB interaction.

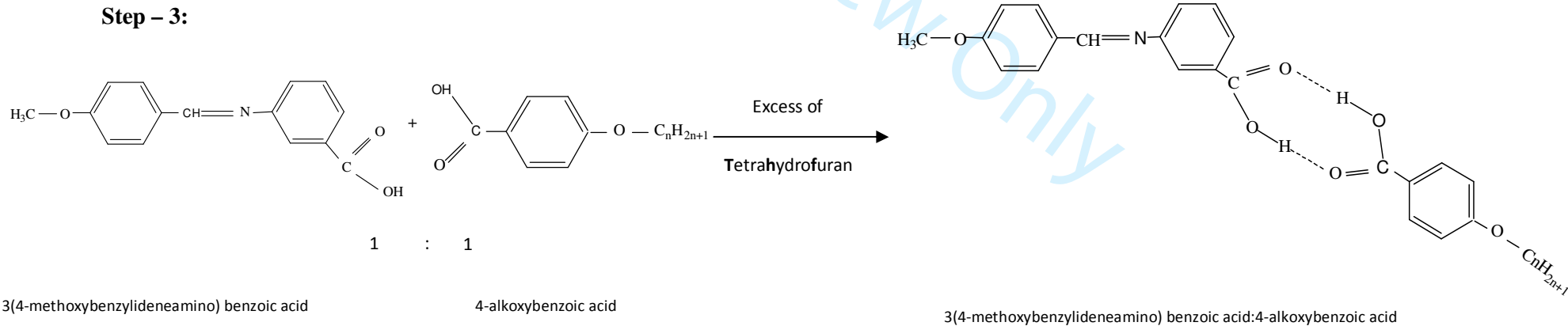
Step – 1:

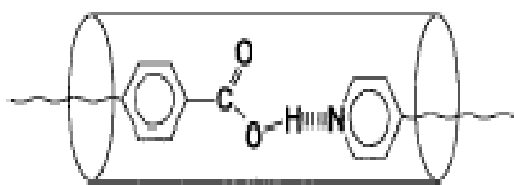


Step – 2:

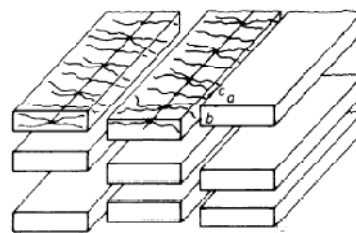


Step – 3:

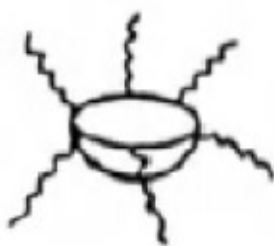




Calamitic



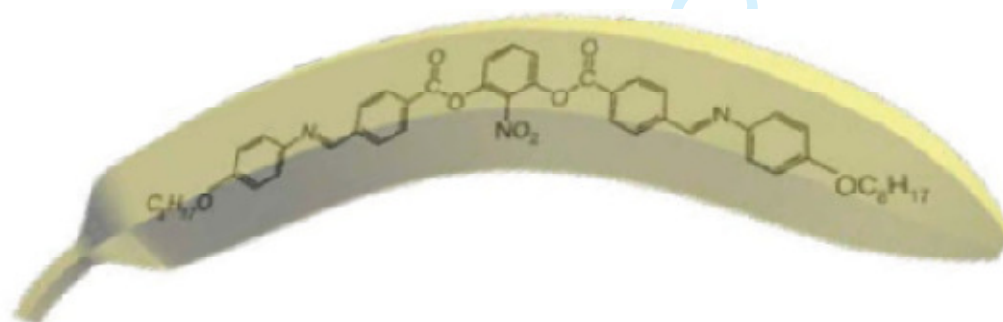
Smectic



Bowl



Discotic



Bent

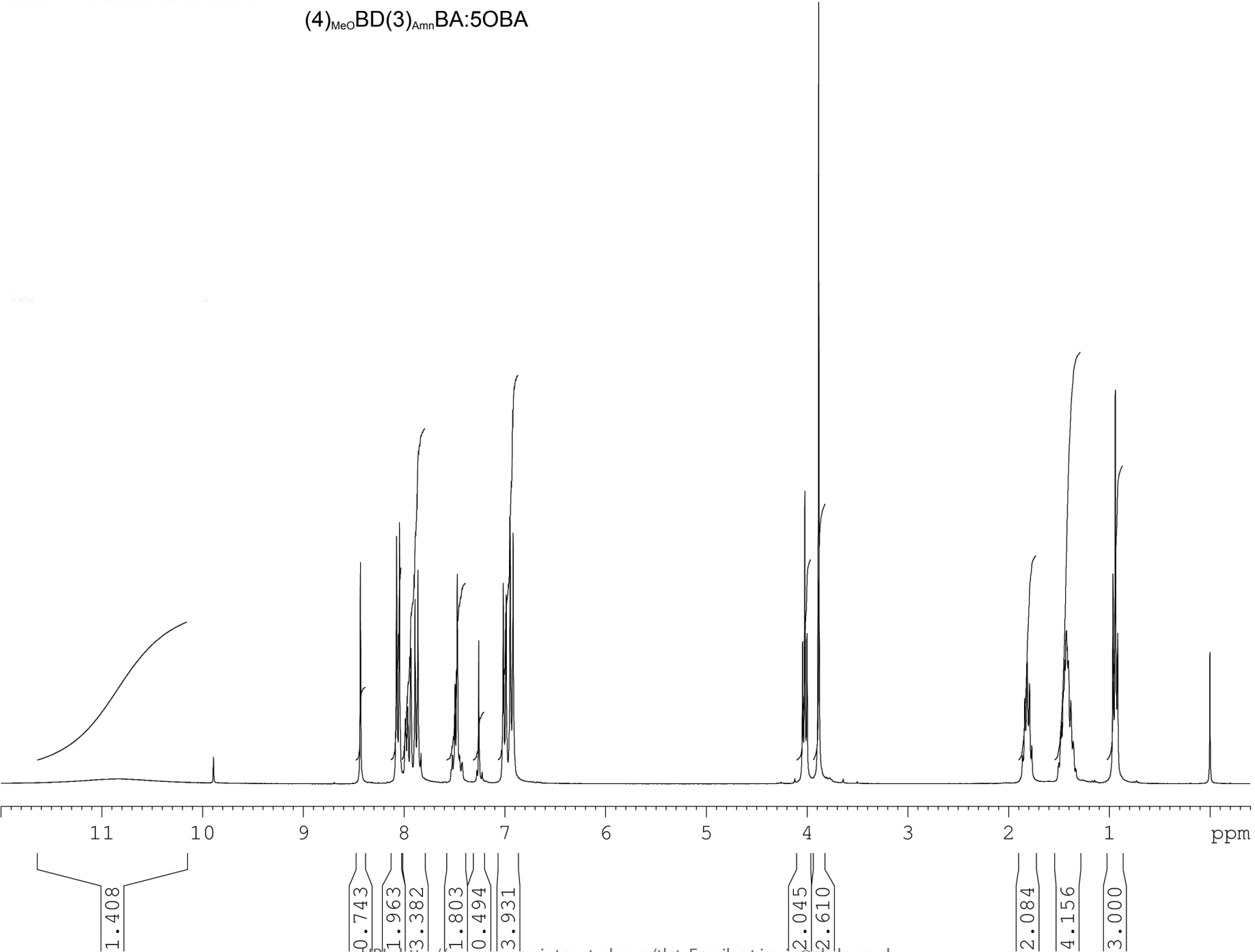


Figure-3

(4)_{MeO}BD(3)_{Am}BA:5OBA

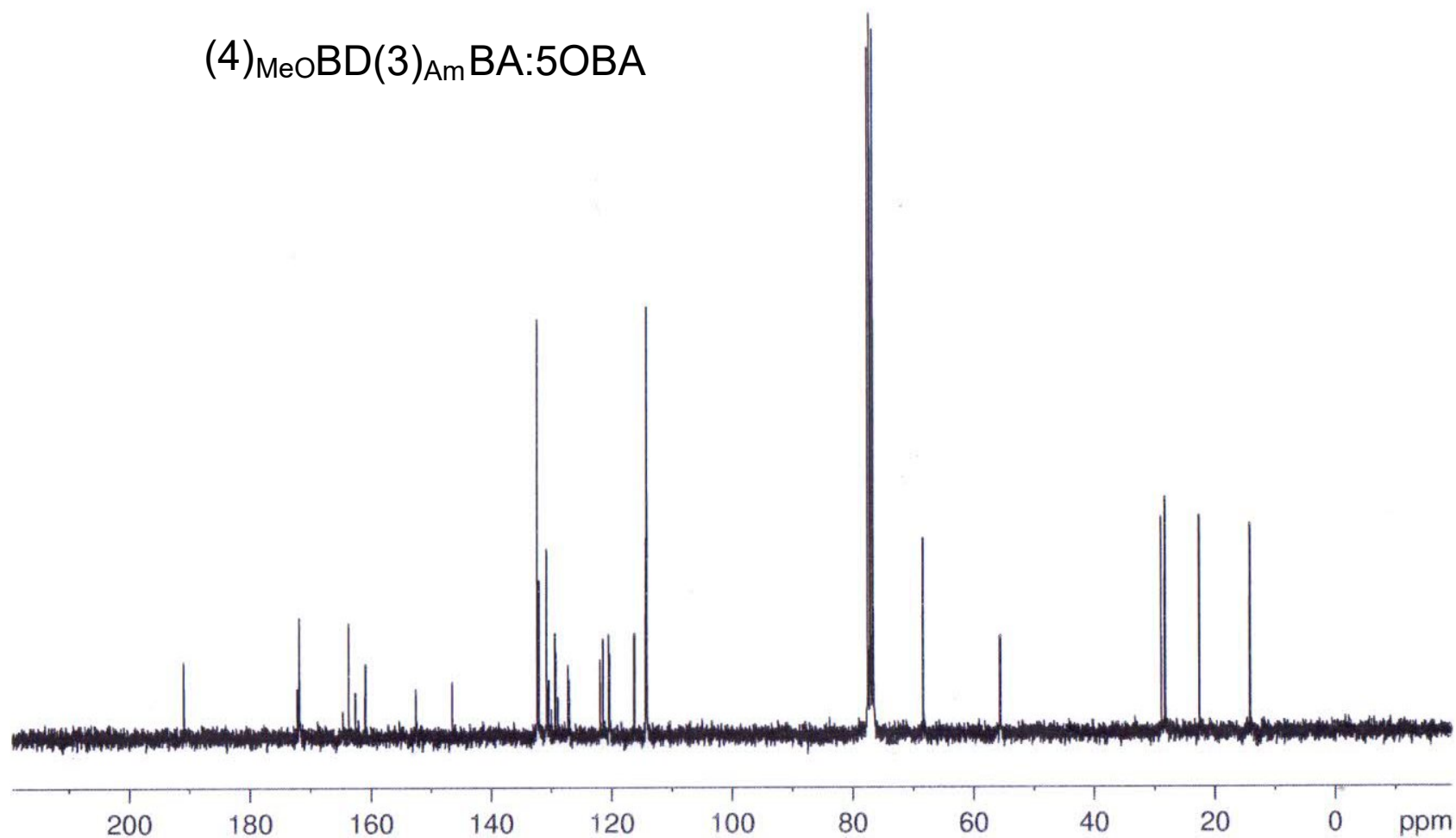


Figure-4

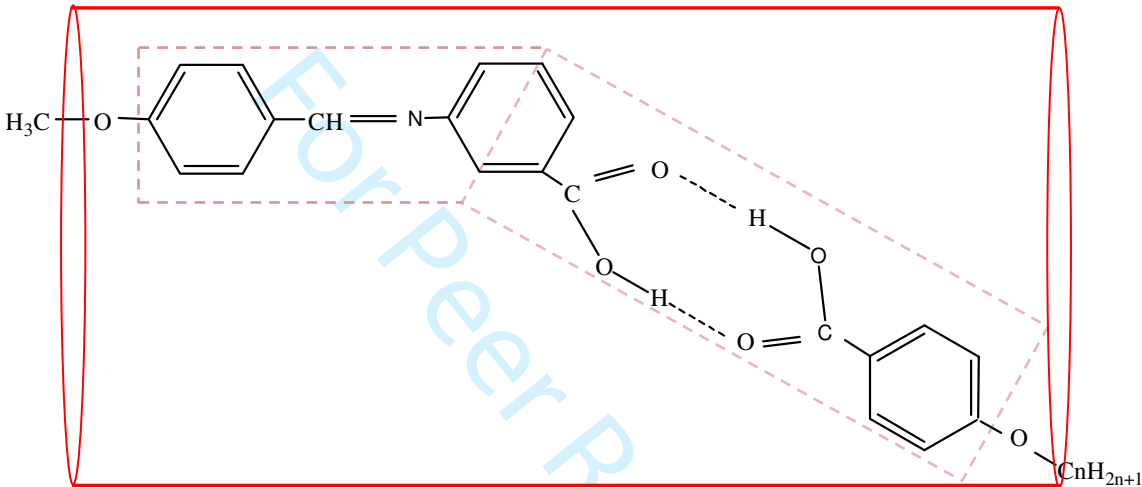


Figure-5a

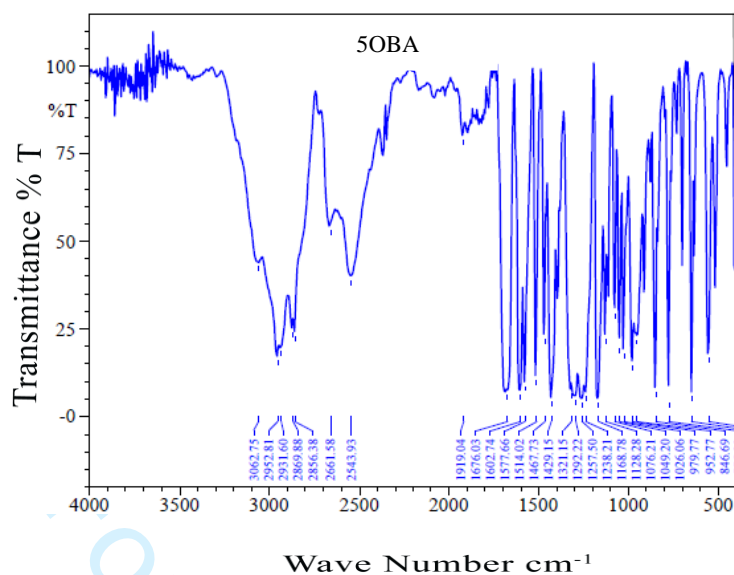


Figure-5b

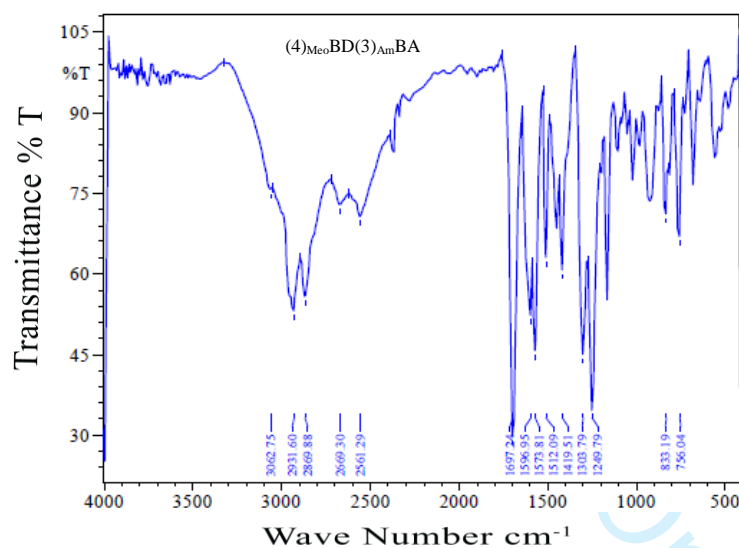
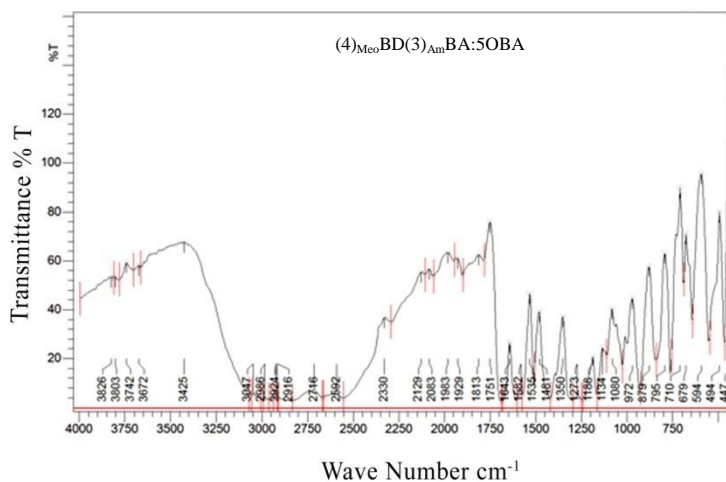


Figure-5c



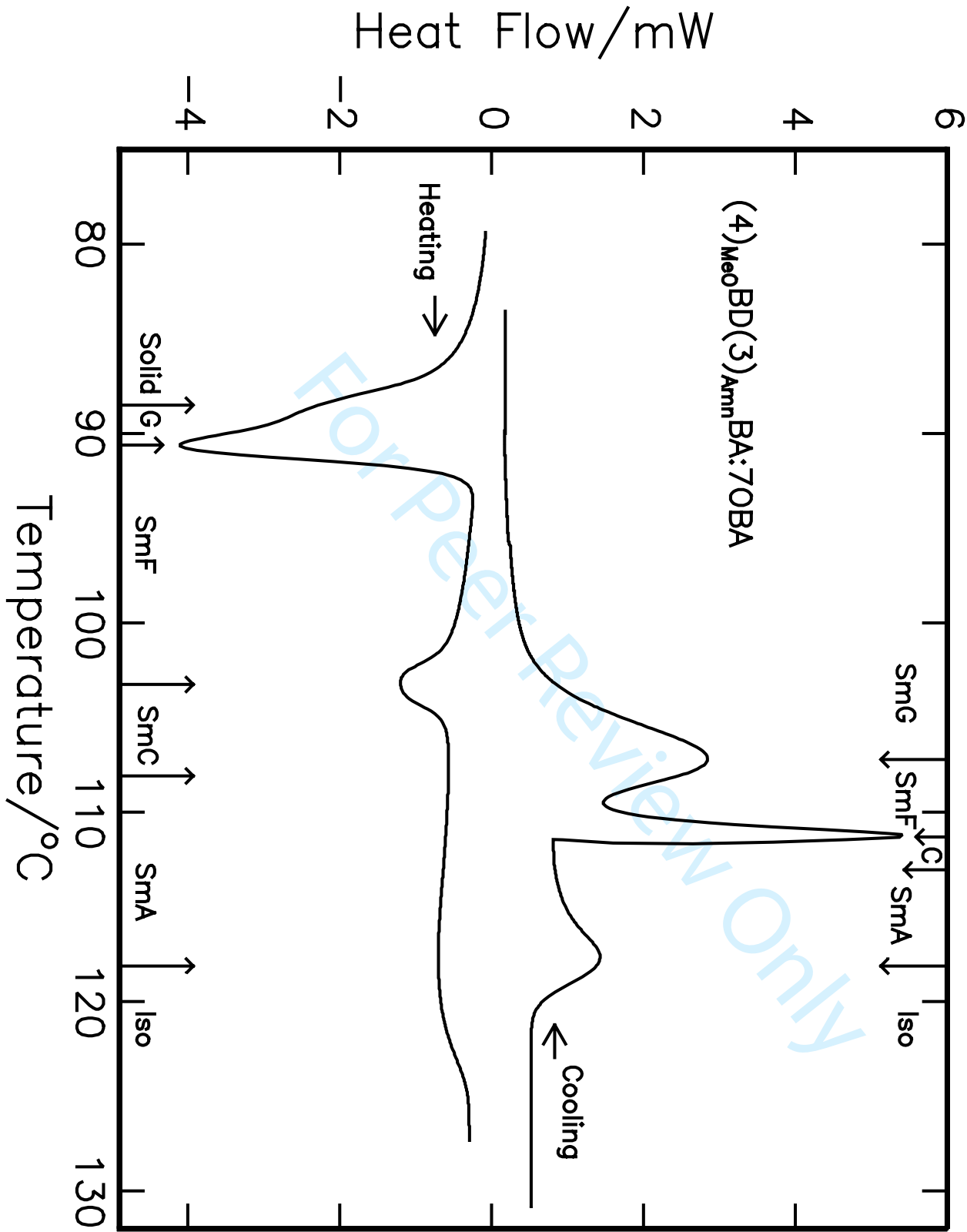


Figure-6

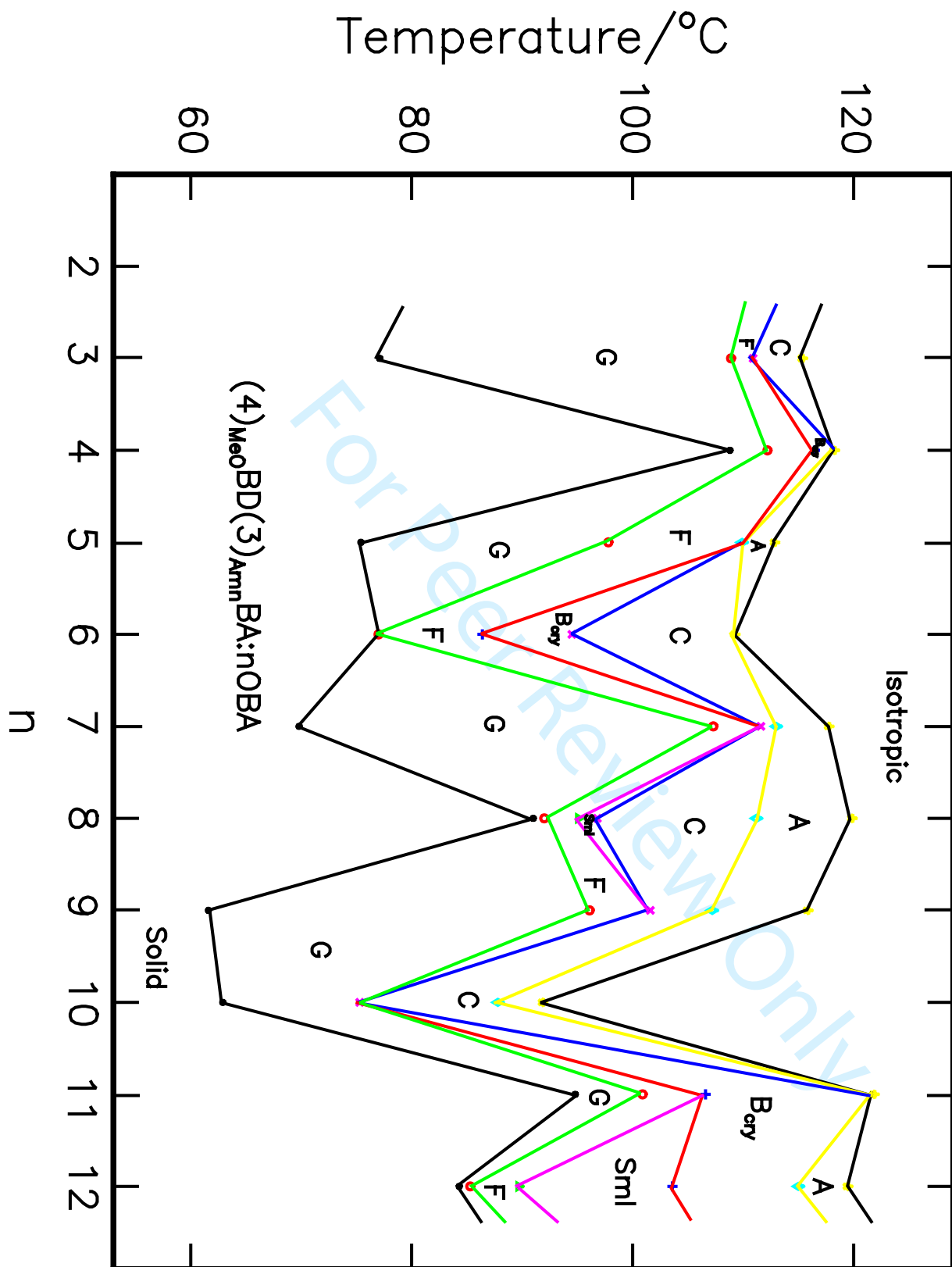


Figure-7

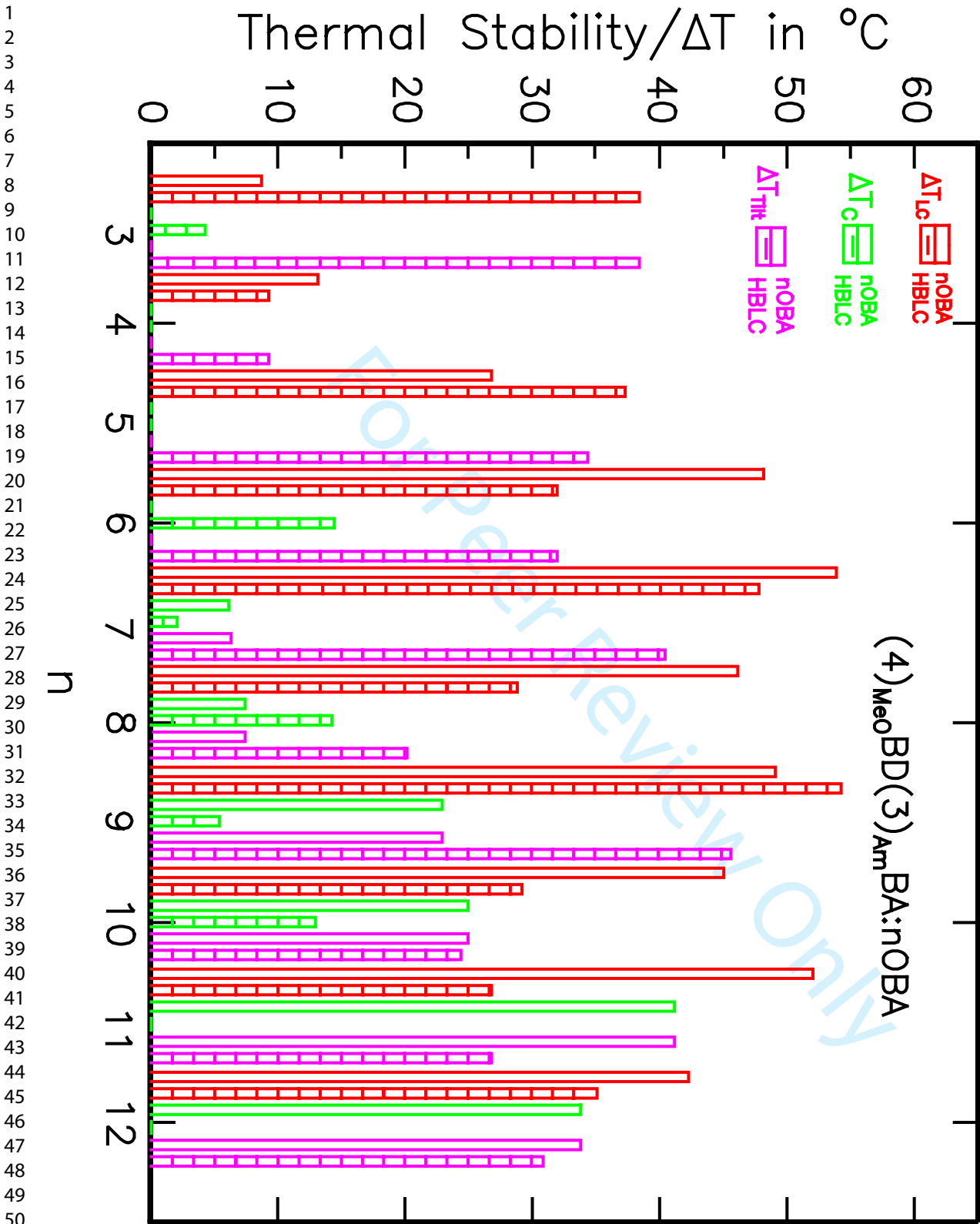


Figure-8

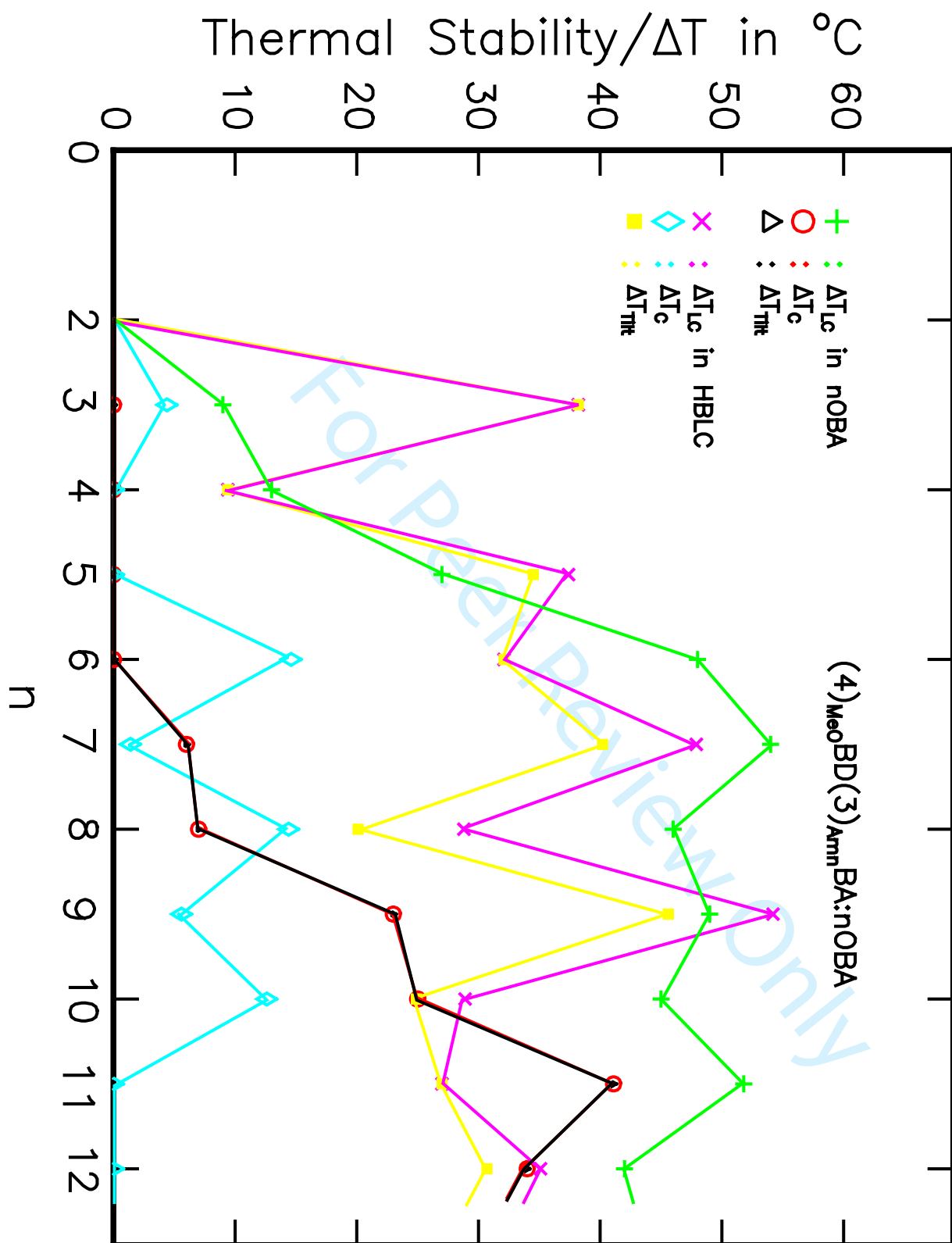


Figure-9

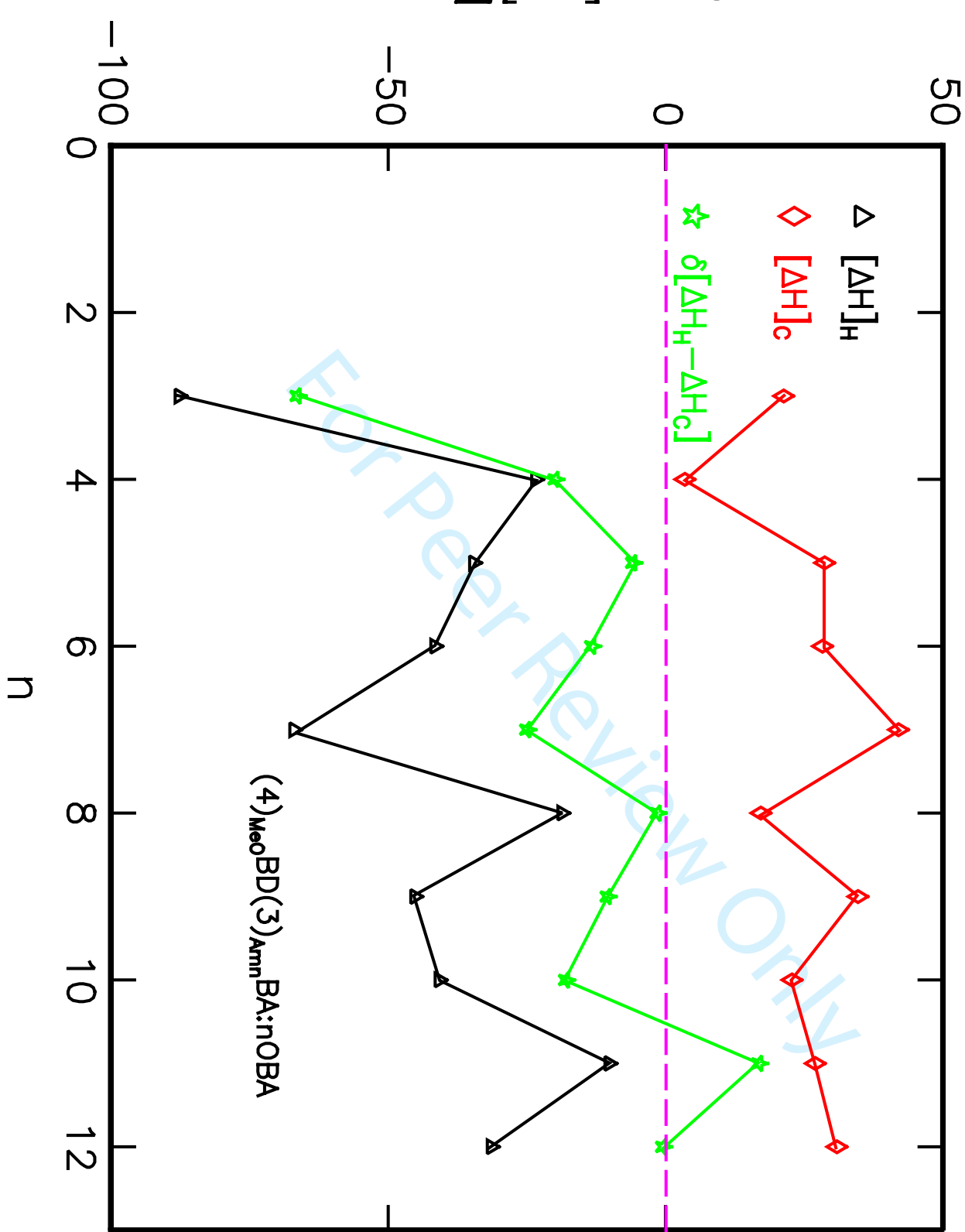


Figure-10

$$\sum[\Delta H] \text{ in J/g}$$

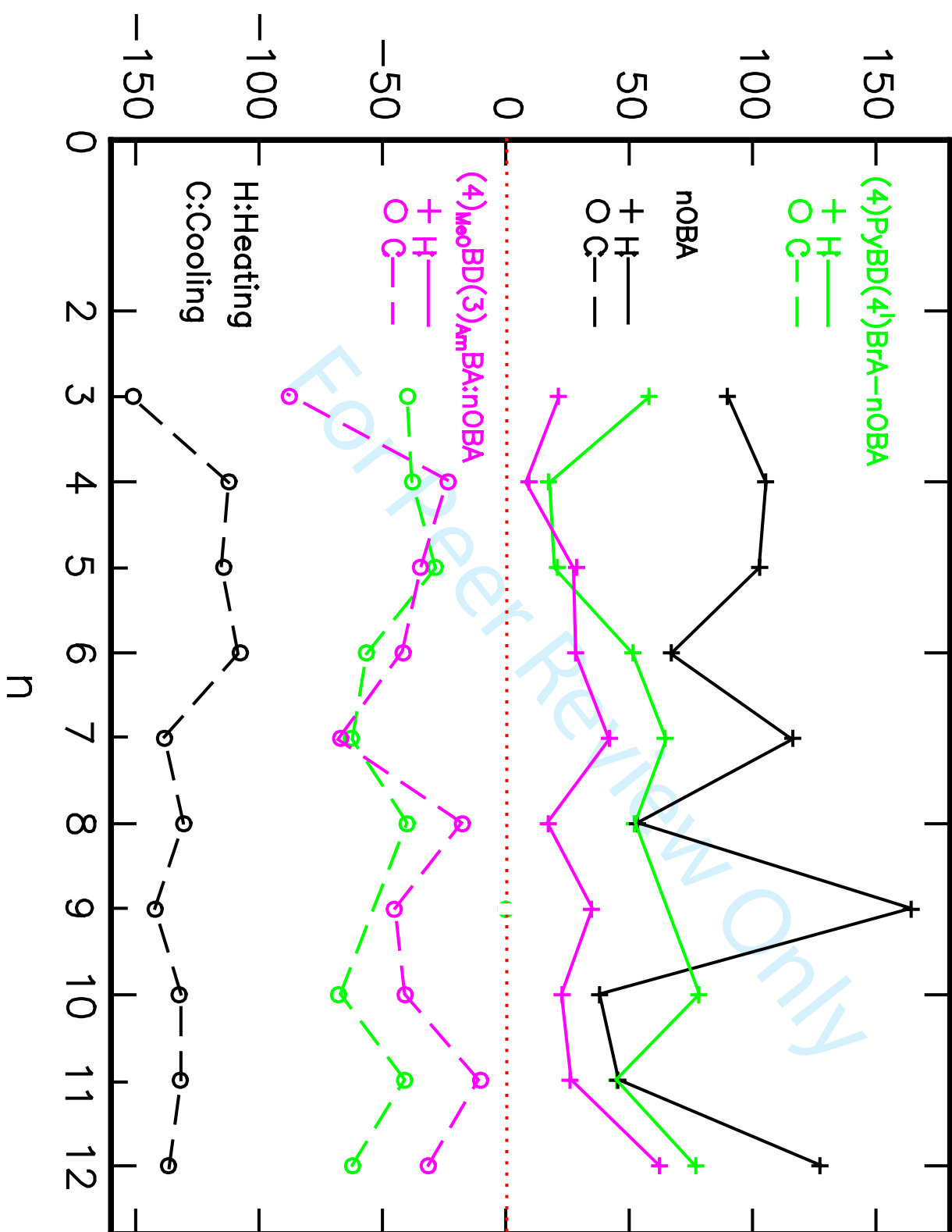


Figure-11

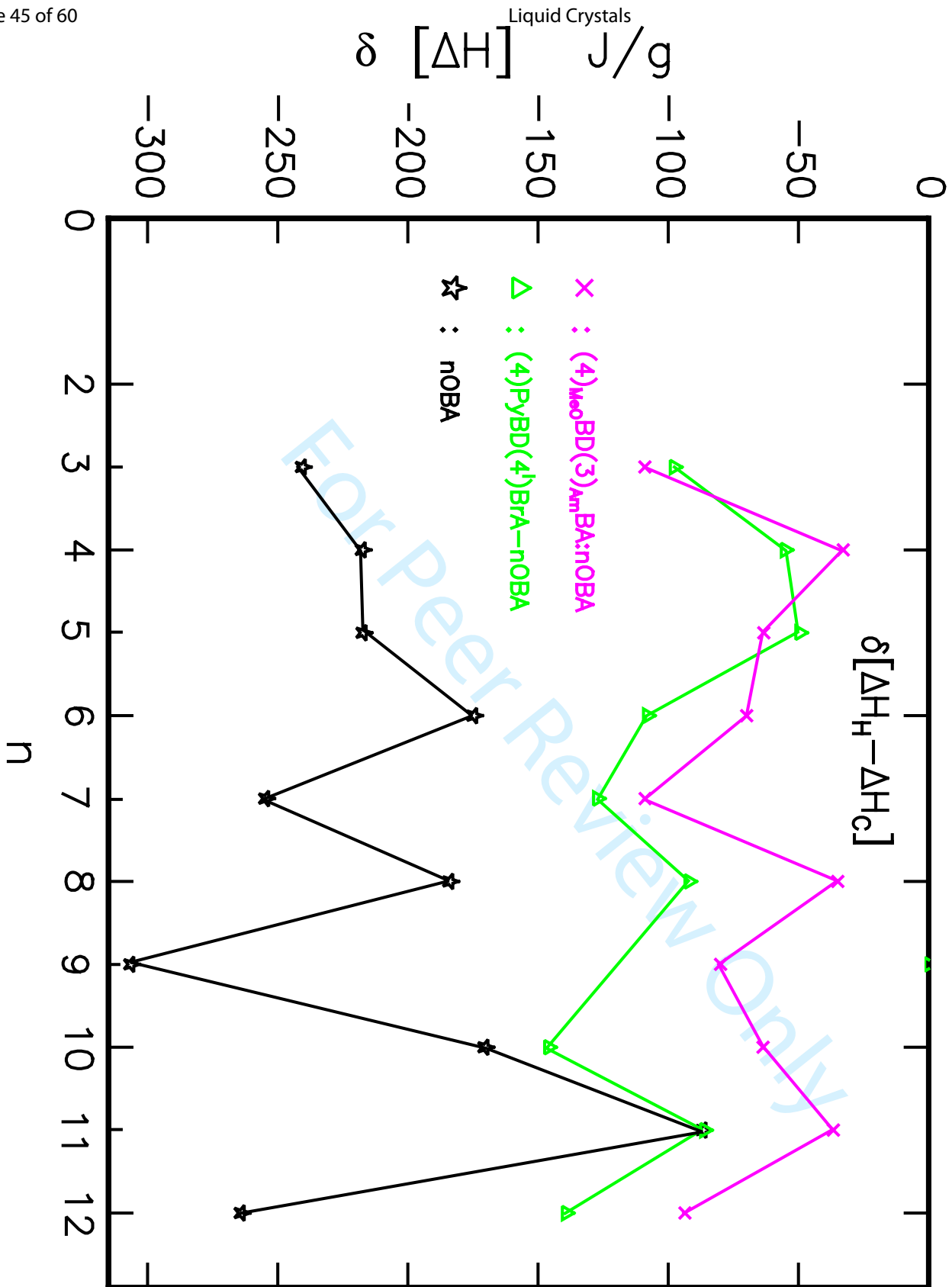
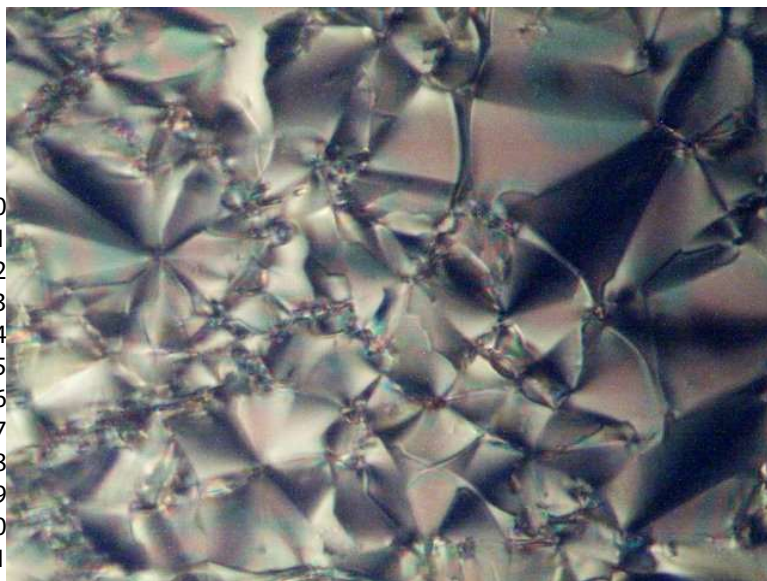
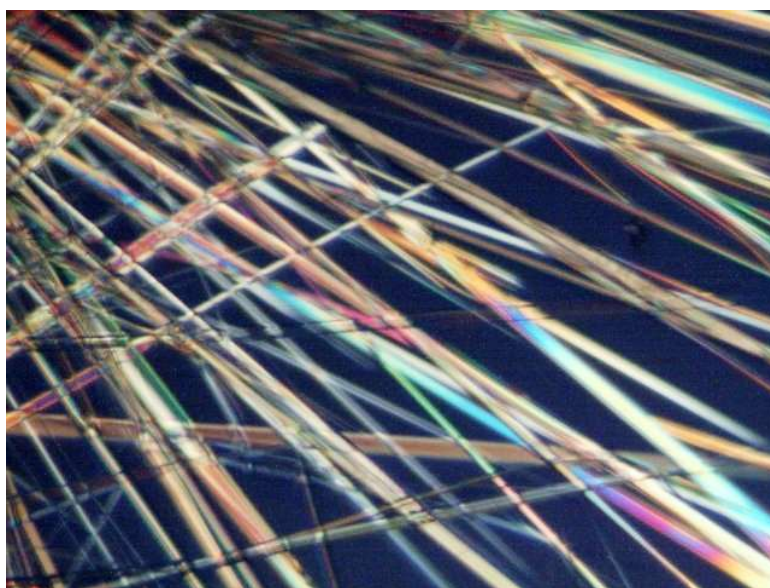
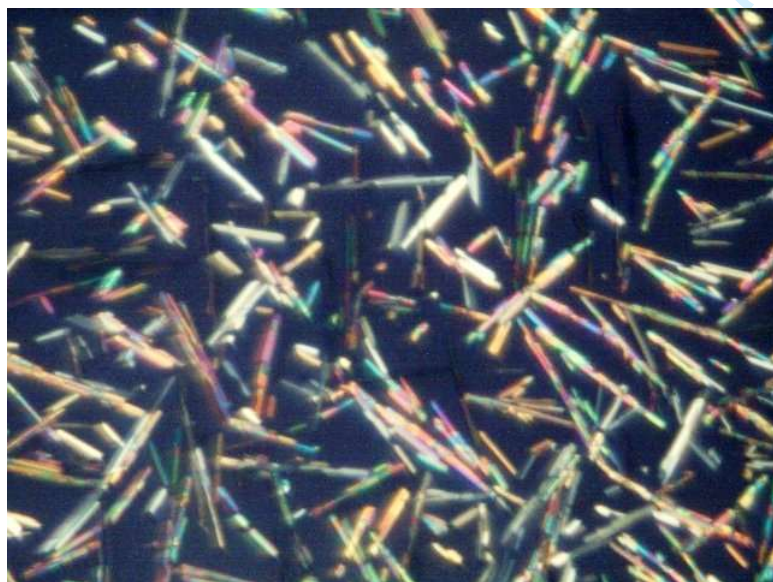
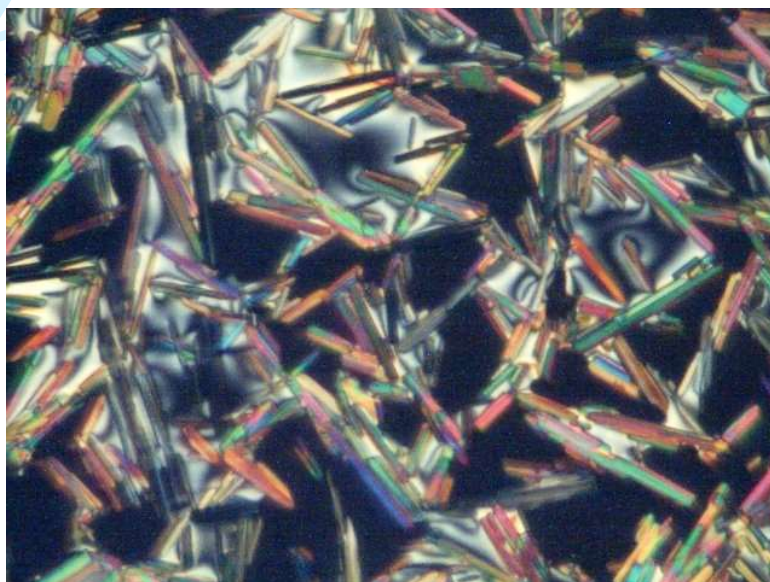


Plate 1**Plate 2****Plate 3****Plate 4**

1
2
3
4
5
6
7
8
9
10
11
12
13
14
15
16
17
18
19
20
21
22
23
24
25
26
27
28
29
30
31
32
33
34
35
36
37
38
39
40
41
42
43
44
45
46
47
48
49
50
51
52
53
54
55
56
57
58
59
60

Plate 5



Plate 6

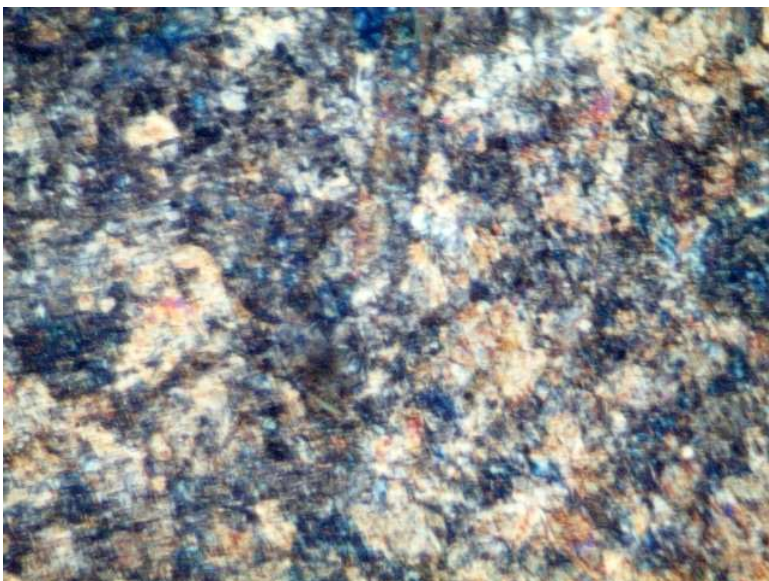


Plate 7

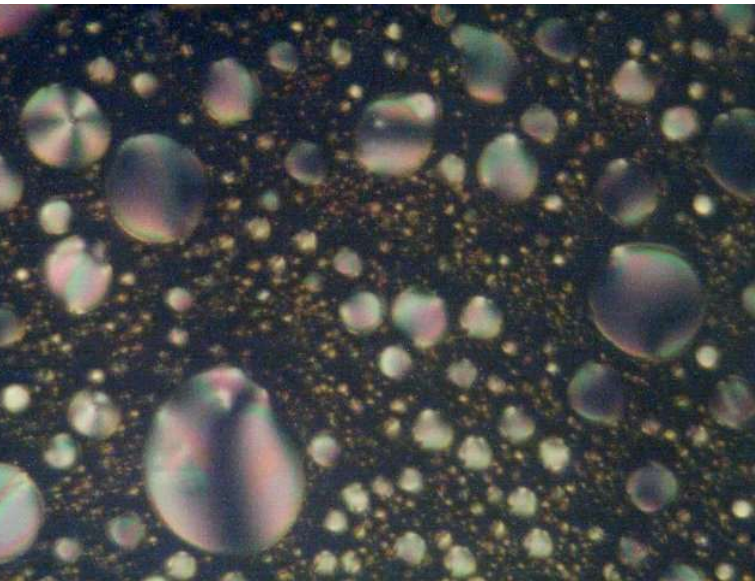


Plate 8

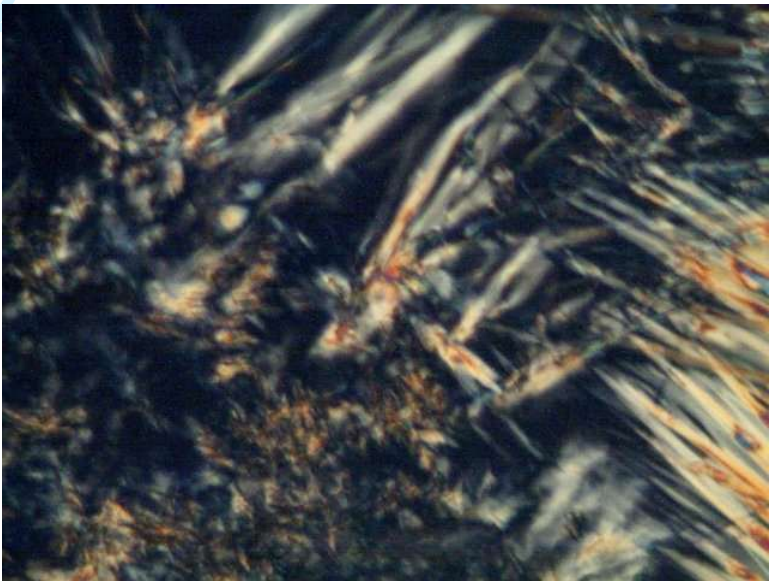


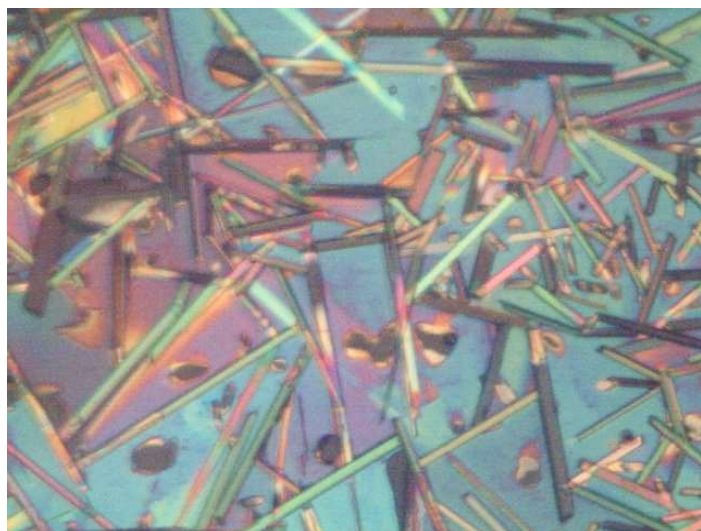
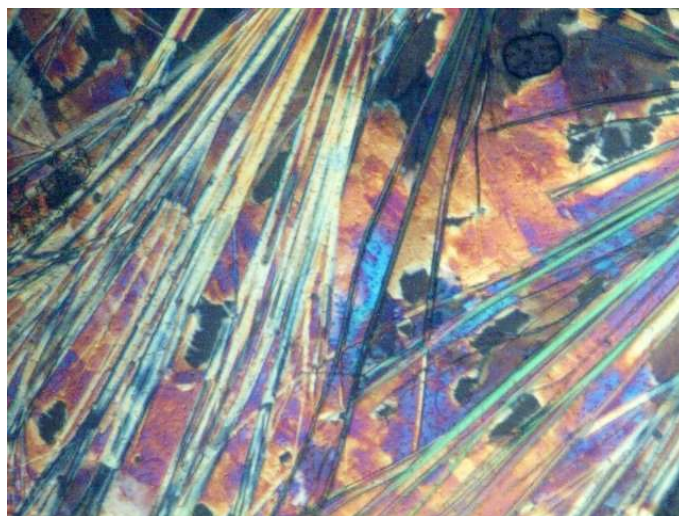
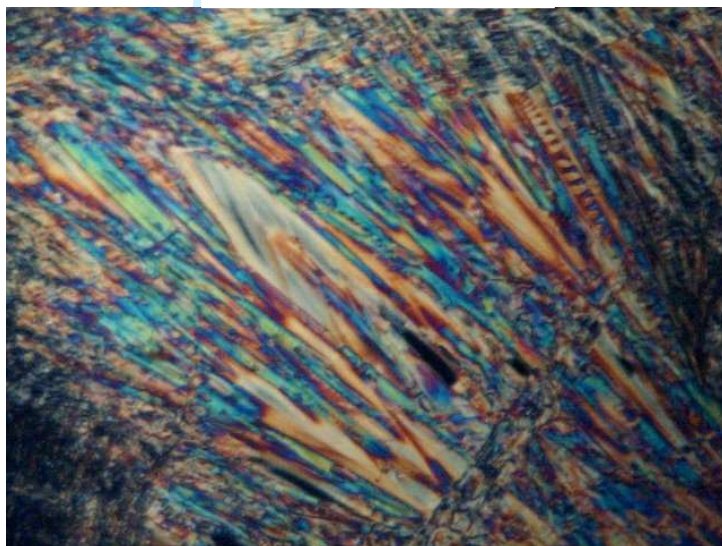
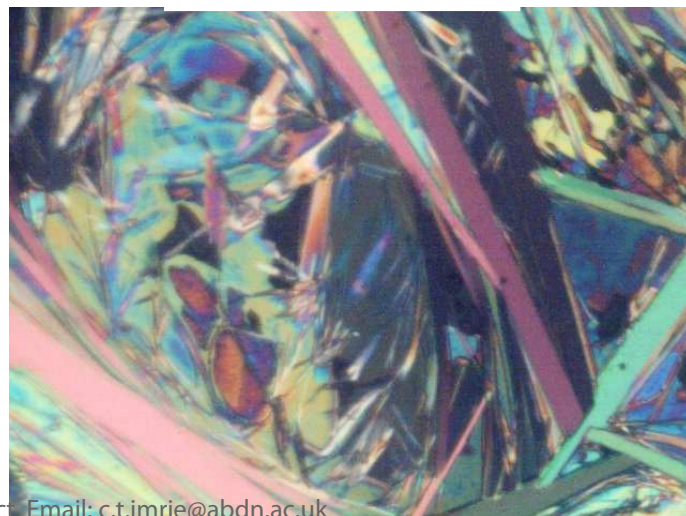
Plate 9**Plate 10****Plate 11****Plate 12****Plate 13**

TABLE – 1

HBLC compound (4) _{MeO} BD(3) _{Am} BA:nOBA for n=	IR Absorption / cm ⁻¹		
	-OH in nOBA	N atom in -CH=N-	Carbonyl >C=O in nOBA
3	2966	1603	1682
4	2955	1603	1683
5	2955	1603	1681
6	2935	1604	1689
7	2934	1605	1686
8	2928	1606	1688
9	2920	1604	1685
10	2916	1604	1685
11	2919	1603	1682
12	2921	1602	1681

Table-2

HBLC (4) _{MeO} BD(3) _{Amn} BA:nOBA	Method		Phase Variance	Details of Transition Temperatures (T _c) in °C and Enthalpy in J/g	[ΔT] _{LC} (in °C)	[ΔT] _c (in °C)	[ΔT] _{TLT} (in °C)	[ΔT] _{OR} (in °C)
3	TM	Heating	G	(RT)SmG→(115.4)→Iso				
		Cooling	GFC	Sld←(77.0)→SmG←(108.8)→SmF←(110.9)→SmC←(115.4)→Iso				
	DSC	Heating	G	(RT) SmG→(115.27)→ Iso [87.65]				
		Cooling	GFC	Sld←(77.08)→SmG←(108.89)→SmF←(110.89)→SmC←(115.27)→Iso [18.14] [2.18] [0.04] [0.94]	38.19	4.38	38.19	----
4	TM	Heating	GFB _{cry}	Sld←(91.4)→SmG→(97.4)→SmF→(113.4)→SmB _{cry} →(118.2)→Iso				
		Cooling	GFB _{cry}	Sld←(108.9)→SmG←(112.2)→SmF←(116.5)→SmB _{cry} ←(118.2)→Iso				
	DSC	Heating	GFB _{cry}	Sld←(91.48)→SmG→(97.40)→SmF→(113.40)→ SmB _{cry} →(118.22)→Iso [1.19] [0.53] [15.86] [5.86]				
		Cooling	GFB _{cry}	Sld←(108.79)→SmG←(112.2)→SmF←(116.52)→SmB _{cry} ←(118.22)→Iso [1.51] [0.12] [1.64] [0.26]	9.43	----	9.43	----
5	TM	Heating	GFA	Sld←(86.0)→SmG→(92.5)→SmF→(104.2)→SmA→(112.8)→Iso				
		Cooling	GFA	Sld*←(75.4)→SmG←(103.6)→SmF←(109.8)→SmA←(112.8)→Iso				
	DSC	Heating	GFA	Sld←(85.71)→SmG→(91.78)→SmF→(104.28)→SmA→(112.81)→Iso [0.63] [0.57] [31.69] [1.71]				
		Cooling	GFA	Sld*←(75.4)→SmG←(97.85)→SmF←(109.87)→SmA←(112.81)→Iso [27.21] [1.1] [0.41]	37.41	----	34.47	2.94
6	TM	Heating	GFB _{cry} C	Sld*←(72.1)→SmG→(91.8)→ SmF→(99.7)→SmB _{cry} →(103.8)→SmC→(109.1)→Iso				
		Cooling	FB _{cry} C	Sld*←(77.0)→SmF←(86.4)→SmB _{cry} ←(94.5)SmC←(109.1)→Iso				
	DSC	Heating	GFB _{cry} C	Sld*←(72.1)→SmG→(91.82)→SmF→(99.73)→SmB _{cry} →(103.86)→SmC→(109.14)→Iso [35.86] [1.47] [0.09] [4.18]				
		Cooling	FB _{cry} C	Sld*←(77.0)→SmF←(86.4)→SmB _{cry} ←(94.5)SmC←(109.14)→Iso [14.02] [0.16] [14.07]	32.14	14.64	32.14	----
7	TM	Heating	GFCA	Sld←(88.7)→SmG→(90.5)→SmF→(103.1)→SmC→(107.8)→SmA→(117.7)→Iso				
		Cooling	GFCA	Sld*←(69.8)→SmG←(107.3)→SmF←(111.6)→SmC←(113.0)→SmA←(117.7)→Iso				
	DSC	Heating	GFCA	Sld←(88.76)→SmG→(90.54)→SmF→(103.13)→SmC→(107.81)→SmA→(117.7)→Iso [41.72] [15.07] [6.69] [0.03] [3.44]				
		Cooling	GFCA	Sld*←(69.8)→SmG←(107.3)→SmF←(111.6)→SmC←(113.0)→SmA←(117.7)→Iso [20.71] [11.34] [0.02] [9.91]	47.90	1.40	40.20	4.70
8	TM	Heating	GFICA	Sld←(92.0)→SmG→(99.5)→SmF→(104.0)→Sml→(107.2)→SmC→(111.3)→SmA→(119.6)→Iso				
		Cooling	GFICA	Sld←(91.0)→SmG←(92.0)→SmF←(95.1)→Sml←(96.8)→SmC←(111.2)→SmA←(119.6)→Iso				
	DSC	Heating	GFICA	Sld←(91.95)→SmG→(99.45)→SmF→(103.86)→Sml→(107.17)→SmC→(111.40)→SmA→(119.76)→Iso [10.93] [1.02] [0.29] [0.53] [0.17] [5.73]				
		Cooling	GFICA	Sld←(91.0)→SmG←(92.0)→SmF←(95.1)→Sml←(96.8)→SmC←(111.2)→SmA←(119.76)→Iso [0.36] [3.77] [1.91] [1.82] [0.01] [9.35]	28.76	14.40	20.12	8.64

9	TM	Heating	GFCa	Sld*←(45.2)→SmG←(92.0)→SmF←(99.7)→SmC←(103.0)→SmA←(115.8)→Iso				
		Cooling	GFCa	Sld*←(61.6)→SmG←(96.1)→SmF←(101.7)→SmC←(107.2)→SmA←(115.8)→Iso				
	DSC	Heating	GFCa	Sld*←(45.2)→SmG←(91.97)→SmF←(99.57)→SmC←(103.02)→SmA←(115.8)→Iso [41.37] [2.03] [0.12] [1.64]				
		Cooling	GFCa	Sld*←(61.6)→SmG←(96.12)→SmF←(101.59)→SmC←(107.18)→SmA←(115.8)→Iso [15.47] [11.05] [0.05] [8.13]	54.20	5.59	45.58	8.62
10	TM	Heating	FCA	Sld*←(49.2)→SmF←(88.7)→SmC←(90.0)→SmA←(91.8)→Iso				
		Cooling	GCA	Sld←(62.9)→SmG←(75.3)→SmC←(87.81)→SmA←(91.8)→Iso				
	DSC	Heating	FCA	Sld*←(49.2)→SmF←(88.7)→SmC←(90.0)→SmA←(91.8)→Iso [6.58] [0.39] [33.81]				
		Cooling	GCA	Sld←(62.9)→SmG←(75.3)→SmC←(87.81)→SmA←(91.8)→Iso [10.92] [3.15] [0.08] [8.70]	28.90	12.59	24.91	3.99
11	TM	Heating	GFB _{cry} A	Sld*←(89.0)→SmG←(92.4)→SmF←(95.8)→SmB _{cry} ←(107.2)→SmA←(121.8)→Iso				
		Cooling	GFB _{cry}	Sld←(94.8)→SmG←(100.9)→SmF←(106.6)→SmB _{cry} ←(121.8)→Iso				
	DSC	Heating	GFB _{cry} A	Sld*←(89.0)→SmG←(92.4)→SmF←(95.8)→SmB _{cry} ←(107.2)→SmA←(121.8)→Iso [1.73] [3.90] [0.97] [3.62]				
		Cooling	GFB _{cry}	Sld←(94.8)→SmG←(100.9)→SmF←(106.6)→SmB _{cry} ←(121.8)→Iso [0.12] [12.68] [6.29] [7.94]	27.00	----	27.00	----
12	TM	Heating	GB _{cry} A	Sld*←(54.6)→SmG←(93.68)→SmB _{cry} ←(102.45)→SmA←(119.36)→Iso				
		Cooling	GFIB _{cry} A	Sld←(84.2)→SmG←(85.2)→SmF←(89.7)→Sml←(103.6)→SmB _{cry} ←(114.9)→SmA←(119.3)→Iso				
	DSC	Heating	GB _{cry} A	Sld*←(54.6)→SmG←(93.68)→SmB _{cry} ←(102.45)→SmA←(119.36)→Iso [30.87] [0.49] [0.03]				
		Cooling	GFIB _{cry} A	Sld←(84.26)→SmG←(85.25)→SmF←(89.73)→Sml←(103.64)→SmB _{cry} ←(114.95)→SmA←(119.36)→Iso [2.04] [15.66] [0.41] [4.3] [7.36] [1.07]	35.10	----	30.69	4.41

*from POM; values in [] indicates Enthalpy in J/g

Authors' Response to Ms. TLCT-2019-0054

Influence of Meta-Extended Rigid-Core, Complementary Hydrogen Bonding and Flexible Chain on Polymorphism in Schiff-based Hydrogen Bonded Liquid Crystals: (4)MeOBD(3)AmnBA:nOBAs.

Krishna Murthy et al.

Authors thank reviewer for his comments which resulted to improve the quality of manuscript. Response to the **general comments** and **particular comments** is partitioned and written in green pen. Accordingly, modified portions of text in the revised script are also marked in green pen. Additional references included in the revised text due to suggestions of the reviewer or circumstantial nature are also listed in green pen.

General comments

The manuscript describes the preparation of new hydrogen-bonded complexes showing liquid crystalline behaviour, a topic of continuous development and interest for the liquid crystal community.

Authors thank reviewer for his encouraging comment regarding the ms. and it's general aspect of interest to the liquid crystal research community.

In this resubmission, authors have tried to clarify the motivation, though the degree of novelty in this approach has not been addressed sufficiently. Some examples of similar supramolecular curved structures could be quoted, as well as future perspectives.

Authors clearly wrote the text for motivation of present work (p-3 & -4, 3rd paragraph in green pen, section-1. However, the sub-heading (as in earlier version) is **removed** in revised version. The novelty aspect of the work is in the revised version addressed (section-1, fig-1, p-4; section-3a, p-6, section-3c, p-10; section-3e, p-13; section-4, p-15 & -16) with respect to the meta-extended core of calamitic type of LC molecules. Nevertheless, the influence of molecular architecture tuned by supra-molecular design involving complementary hydrogen bonding interaction is also analyzed. The type of hydrogen bonding is also mentioned in the title of paper. Influence of meta-extended core and complementary HB for the realization of device savvy tilted LC phases constitutes the overall contributory aspect of the present work.

There are still quite a few style refuses and paragraphs are definitely too long. There is still too much fundamental information. The ideas are difficult to follow and some figures hard to read. The paper could be simplified to attain a higher impact and visibility, highlighting the main ideas (how to maximise SmC and other tilted phases).

Long paragraphs in the old script are partitioned (section-3c, p-8 & -9; section-3d, p-10 & -11; section-3e, p-12, -13 & -14; section-3f, p-14 & -15) in revised version by highlighting the impact of meta-extended LC core and supra-molecular HB architecture for the enhancement of SmC and tilted LC phases.

Fundamental, but, redundant information regarding the DSC peaks to identify T_c and evaluation of ΔH etc., in removed in the revised version.

Clarity of ideas and its readability for ms. are improved by re-writing (p-4; p-6; p-8 & -9; p-11; p-12 & -13; p-15 and p-16) the text. Modifications are incorporated in some figures (old fig-7 is redrawn as Fig-9) to for improve clarity. Additional figures (Fig-11 and Fig-12) are also included to explain the trends with improved clarity.

Considering that the findings are potentially interesting for the journal readers, my recommendation is that the manuscript can be accepted for publication in Liquid Crystals, but only after major corrections are carried out, including, considerable re-writing and restructuration.

As per the reviewer's directive, a major revision is carried out with corrections, re-writing and restructuration to bring out a comprehensive overview for the impact of meta extended core for the LC phase abundance. Modifications are marked in green pen.

Authors should still consider previous comments on figures and tables, as well as a new set of particular issues that are now presented.

Reviewer's earlier comment to increase the clarity for figures and tables is taken care in the revised version. Fig-1 is newly introduced. Fig-4 is a revised version of old fig-7 that conserves the clamitic shape of HBLC complex, despite it being superposed by bent (meta-extended core) shape. Fig-5(a,b,c) represents redrawn old fig-3(a,b,c) with uniformity for X-axis and notation for wave number duly inscribed. To improve the clarity, readability and contrast, trends in ΔT_C and ΔT_{Tilt} of nOBA's in old fig-7, are redrawn as Fig-9. New illustrations, viz., fig-11 and fig-12 are also introduced in to the revised script in respond the reviewer's comment of section-3 (p-13 of old script).

Particular comments

Abstract.

Avoid acronyms that have not been introduced earlier.

Abstract is revised by giving full expansion for acronyms. The acronym 'HBLC' in abstract is provided (p-1) with full expansion in the revised script.

Corrections for the text (lines-28 and -30 of old script), which are required as per the experimental observations are also incorporated in the revised version. Correction is made for line-34 (of old script) as many multicritical points are identified in the phase diagram.

Introduction

Page 4. Line 22. I would eliminate "Motivation:"

The subheading 'Motivation' is deleted (p-3 and -4) from the text of revised version.

Page 4. Line 22. "Selection of Oxygen atom as bridging moiety and Schiff base as core are known to promote lateral stacking and growth of layered smectic phases." Does require a reference as evidence? Possibly it appears later.

References for the Schiff base moiety [17,19,25,31,32] with Oxygen as bridging atom [18,19] and its influence to enhance lateral stacking trend (viz., for induction and origin of layered smectic phase structures) are included (p-3 and -4) in the revised script.

Page 4. Lines 35 to 45. Please consider rephrasing, in order to clarify what the aim of the study is. I also suggest to include a molecular sketch of the complexes formed.

Aim of the present study is rephrased (p-4) for clarity in the revised text. In accord with suggestion, a sketch for the HBLC complex (fig-4) is also included in the revised text at an appropriate (p-6) place.

Page 4. Line 47. Add "A" at the start of the line.

As correctly pointed out by the reviewer, an indefinite article (An) is used (p-4) to initiate the sentence.

Page 4, Line 3. "Influence of HB and its type are investigated using the results of POM and DSC." Probably not needed.

Probably, the reviewer might have mistyped as p-4 and line-3, instead of p-5 and line-3 of old script. It is understood as a case of redundancy, and with this in view, this sentence is deleted (p-4) in the revised script as per the suggestion of reviewer.

Page 5. Line 7. . The whole paragraph seems a bit redundant.

"Paper is organized in **three** sections. Details of chemical constitution and influence of HB for the occurrence of device relevant LC phases are presented as introduction. Motivation for the targeted work is also presented in the section-1. Selection and procurement of chemical ingredients, synthetic route and details of experimental techniques are presented in section-2. Discussion for observed trends and their analysis are presented section-3"

Cited paragraph is simplified (p-4) as one sentence to detail the organization.

Section 2.

Replace "ingredients" by "reactants".

As suggested, the term – 'ingredients' is now replaced (p-5) by *reactants* in revised version.

Page 5. Line 37. "The product obtained in the 1st step which is found to be white in colour signifies its purity." If NMR is clear, colour needn't to be a purity criteria.

White (or more appropriately colorless) product formed is generally advocated to vouch the initial purity of sample, or else, it's immunity against the possible chemical degradation. Text is modified (p-6) in the revised version in the context of this spirit.

I suggest to include "Techniques" before and the "Synthesis", then stating in this section that the Structures were verified by NMR and FT-IR.

As suggested, the words, viz., *Techniques* and *Synthesis* (sections-2a & -2b) are included in the revised script.

Section 3.

Following my previous comment, from my view, the discussion from Page 6. Line 53 until Page 8. Line 50 should be Supplementary information.

Data for ^1H -NMR and ^{13}C -NMR chemical shift, relevant figures and its discussion (at least for one representative out of entire series consisting of 10 compounds) is an accepted practice for this journal. In response to the earlier comments, the data of chemical shift is already shifted to Appendices-A and -B. As per the suggestion, along with the data of chemical shift and tally of H- and C-atoms by the analysis of representative figures is also shifted to the appendices in the revised script. The option of whether –

a) to retain data, figs and discussion (for tally of C- and H-atoms) in Appendices-A and -B or
b) to push in to the supplementary section

is left to the decision of editor. Since discussion for the account/tally of H-atoms and C-atoms provides a clinching evidence to confirm the formation of targeted HBLC complex, authors strongly opine for the retaining (p-5) the NMR representative figs-2 & -3 in the main text and relevant tally of H- and C-atoms in (p-27-32) appendices.

Page 6. Line 33. I would rename this section as “Complexes structures or formation”, since the molecular structure corresponds to section 2. (in any case “Supramolecular Structure”). I would then include the FT-IR discussion, to assess the complex formation.

As suggested, section-3a is renamed (p-6) as “Supra-molecular Structure of HBLC Complexes”, while the FTIR discussion follows.

Page 8. Line 52 and following. The FT-IR discussion is now more convincing, and well sustained. Authors should consider using Fig. 3(a) and 3(b) for the pristine components, then Fig. 3(c) for the mixture (for the sake of argument). Authors should also consider shrinking this paragraphs considerably, to keep a sensible size of the paper.

Figures 3(a), 3(b) and 3(c) are still a bit unclear, and Fig. 3(a) needs wavenumber annotations (for the sake of consistency).

As suggested, old figures-3a,b,c are renumbered as figs-5a,b,c and re-organized, such that 5a and -5b correspond to pristine components, while -5c is earmarked for the end product HBLC complex. Shrinking of paragraphs pertaining to IR discussion seems difficult, to hold the integrated and comprehensive outlook of discussion.

Modified figures (-5a,b,c) are clearly annotated with wave number to maintain the consistency. Additionally, consistency of scaling for X-axis (keeping minor ticks) is also preserved throughout the new Figs-5a,b,c. However, since IR absorption for fig-5c seems to get superposed with X-axis scaling, additional version of figs-5a, -5b, and -5c are submitted as supplementary (figs-5a,b,c) information.

Authors are encouraged to merge these three in the same figure, by piling up the curves and shifting them towards the Y-axis.

As per reviewer’s suggestion, all the three (-a, -b, and -c) curves are piled up as one figure-5 in both of the versions.

Page 11. Line 5. “LC phases are identified by their comparison with standard POM textures reported”, is this needed, or simply common knowledge?

As suggested, the sentence is removed in revised version.

P11. Line 17. “Similarity of molecular architectures between the present meta-extended core and the one side mass loaded core (with double chiral centres) is argued to result for the textural similarity.” Specify reference.

As suggested, the relevant references, viz., Refs.-69, -70 are included (p-9) in the text of revised version. They are listed in the reference section also.

P11. Line 21. The following text could appear as a separate paragraph, or could be summarised with the information of the phase assignation, leaving the textures description as SI.

“SmC phase is found to exhibit four brushed schlieren texture (plate-4) as grown from the precursor SmA phase in heating run of (4)MeOBD(3)AmnBA:8OBA. SmC phase is found to exhibit blackonwhite natural mosaic texture (plate-5) also. SmBcry is found to grow as colored mosaic (plate-6) and glossy focal conic fan batonnet textures (plate-7). SmI is found to exhibit broken focal conic plume-like fan (plate-8) texture when grown by cooling the SmBcry in (4)MeOBD(3)AmnBA:8OBA. SmI is also found to

exhibit colored threaded (plate-9) texture in (4)MeOBD(3)AmnBA:12OBA. However, SmF is found to exhibit characteristic colored marble threaded texture (plate-10) and checkered board of elongated fan textures (plate-11) in HBLC complex for n=9 and 12, respectively. In addition to the above textures, SmF is also found to exhibit a paramorphotic colored mosaic texture with undulated boundaries (plate-12). This texture is found to be much akin to the undulated edge texture observed for n=11 in the cooling run. SmG exhibited characteristic colored mosaic (plate-13) texture in the lower homologues of the present series of HBLCs."

Since, this paragraph (section-3c, 2nd paragraph, p-8&9) entails continuity of discussion for POM observations (i.e., from plate-1 to -13), authors opine that splitting the paragraph would be improper. Inability to comply with reviewer's opinion may be comprehended as an effort to bring a comprehensive view and integrity to the text for POM observations.

However, in accord with the suggestion of the referee, summary of POM textural observations and the phase variance with respect to the molecular architecture is scribed as separated paragraphs (p-8 and -9) for clarity.

Authors may be given an opportunity to express and submit their objection to shift POM textures and relevant discussion in to the supplementary information file. After all, POM textures court the fulcrum and fundamental experimental evidence to confirm the occurrence of LC phases with a variety and diversity of structural/orientational orders.

P12. Line 7. Please clarify/rewrite this text:

"Although intermediate and higher homologues do not exhibit 3D SmBcryst phase, the lower homologues are found to exhibit orthogonal (hexagonal) SmBcryst phase. But, higher homologues (for n=11 and 12) are found to exhibit SmBcryst again."

Cited text is re-written (p-8 and -9) to improve the clarity in the revised version.

P12. Line 19. The text below is an interesting observation. Can the authors specify what conditions promote the appearance of tilted phases in nOBAs, and compare to the present complexes (perhaps as a function of alkyl chain length "n")

"Overall tilted phase abundance in HBLCs is observed to witness an enormous amount of increase in comparison with nOBAs. Hence, meta extended LC core is argued to promote tilted phase stability for device applications."

Last sentence of 1st paragraph of p-9 is also re-written to specify the conditions that prevailed for the appearances of tilted LC phases. Especially, the influence of meta-extended core and increased flexibility (by end chain length "n") are also included to justify the observations.

Page 12. Line 30. Not sure this is needed:

"Temperatures at which DSC thermo gram exhibits a dips (in heating scan) or peaks in cooling scan is identified as phase transition temperatures."

As per reviewer's directive, line (p-10) is removed in revised version.

Page 12. Line 24 to Page 13 Line 36.

Authors are strongly suggested to break down this paragraph into three main topics, and simplify the discussion:

- General description of DH and Ti values (comparison with literature).
- Small enthalpy changes associated to small structures of tilted phases.
- Monotropic character of the longer-chains analogues.

I would shrink the text and refer to the tables.

Entire paragraph of old version is split in to three paragraphs (p-10 & -11) with different side-headings (subsections-3d_{i,ii}) as suggested by the reviewer.

In the revised version, i.e., section-3d(i), the shifting trend of LC phase range towards ambient temperatures due to the meta-extended core and complementary HB is also introduced in p-10.

Page 13. Line 38 to line 51. The paragraph can be considerably reduced, as it is clear that increasing the alkyl terminations may tune the flexibility. It'd be more interesting to actually compare a similar variation in "n" on other systems (nOBAs, for example).

Reviewer's comment is properly responded by the authors. And so, effort in this direction yielded finer aspects of influence of molecular design. As suggested, the interesting aspects of variations of flexible alkyl chain length (n) in meta (table-2) extended HBLC's and in pure [10] dimeric nOBA's is introduced in the beginning of section-3e in p-12 and -13 of revised script. The impact of meta-extended LC core now clearly exemplifies enhanced abundance of device savvy tilted LC phases.

Page 14. Lines 17 to 46. Text appears repetitive and could be merged as part of the introduction, then focus on the results in this (already) long section.

As suggested, the seemingly repetitive text is shifted in to the introduction (section-1, p-4).

Some redundant part of the text is also removed.

Page 15. Line 21. To my view, this sentence is not clear, considering that nOBAs are indeed HBLCs:

" ΔT Tilt is found to be zero for $n \leq 6$ in pure nOBAs, while it is found to attain a finite value in HBLCs to infer the influence of HB for inducing tilted LC phases."

The sentence is rewritten (2nd paragraph, p-14) in the revised version to improve the clarity.

Please rephrase the following sentences for clarity:

Page 15. Line 52. "SmC phase stability $[\Delta T]_c$ is found to exhibit almost a monotonical increase for $n \geq 6$ in (except for the increment of $n=11$ to $n=12$) than in pure nOBAs. But it is also observed that the $[\Delta T]_c$ attains higher values for even homologues in HBLCs."

Sentences regarding the discussion of $[\Delta T]_c$ is rewritten (p-15) with improved clarity.

Page 16. Line 11. "It is also noticed that $[\Delta T]_c$ is found to attain either a lesser value or zero value for all odd homologues with $n \geq 4$ for HBLCs"

Sentence is rewritten (p-15) for clarity regarding the contrast behaviour of $[\Delta T]_c$ in odd homologues of meta-extended core LCs.

Page 16. Lines 11 to 34. This discussion requires major polishing, trimming and organising. (check the typo in $5 \geq n \leq 11$). I suggest that just a few ideas are shown, expressing clearly when the discussion refers to nOBAs and when to the new complexes, considering that both series are HBLCs.

Cited text (Page 16. Lines 11 to 34 of old text) by the reviewer is re-written (p-15) with enhanced clarity in the revised script by considering the contributions of μ_i for meta-extended core, inclined HB interaction and orientational disorder by odd homologues. Typographical mistake for greater/lesser inequality is corrected in revised version.

Page 16. Line 32. The following paragraph looks contradicting?

"LC phase stability with the underlying structural diversity is found to be maximum for $n=9$ and 10 compounds. The observed higher LC phase stability for the $n=7$ and 9 is argued due to the chain number being odd in these compounds."

In accord with reviewer's previous directive, text (p-15) is re-written to eliminate the alleged

contradiction is eliminated.

The whole page 16 is one single paragraph, which makes following the ideas rather difficult.

Entire paragraph is split (p-15 and -16) into three small paragraphs and sentences are restructured. Almost entire text is re-written to improve the clarity by comparing with nOBA's and meta-extended core LCs.

Page 16. Line 53 and following. Almost all section 3h is stating the evident, including the physical meaning of phase transitions. I personally do not see what the contribution of this section is.

Old version of section-3h is now re-written as section-3f. The contributory aspects of comparative study (through figs-10, -11 and -12) of integrated and differential enthalpies is to emphasize the impact of meta-extended core design on the growth of LC phase structures optimized over the heat energy exchange during heating and cooling scans. Sumptuous amount of discussion is introduced in the re-written text (p-16 & -17) in the revised script.

In fact, reviewer's comments regarding

a) contributory nature of the fig-10 with discussion of integrated enthalpies and

b) influence of meta-extended architecture

c) exclusion/isolation of HB interaction

d) inclusion of Schiff base LC architecture

rendered the authors to introduce figs-11 and -12 for to carve out a meaningful text in the revised text.

Conclusions.

As a general comment, I would avoid bullet points.

As suggested the bullet point version is changed (p-15) in to a single paragraph for conclusion.

Page 17. Line 41. I would rather say "preparation" than "synthesis" of the new HBLC.

As suggested, the term "synthesis" is replaced (p-17) by "preparation".

Bullet point i) The phrase does not make sense, but, in any case, the complex formation is assessed by FT-IR.

Authors modified the text regarding spectroscopic methods. The first two sentences (in conclusions, p-17) are written as to how these methods can be used to confirm the formation of targeted HBLC complex.

Bullet point ii) is not clear. The effect of extension of supramolecular core should be clarified, and also, "extended" with respect to what? Respect to the nOBAs? Some examples on other supramolecular liquid crystal having curved geometries and resulting dipoles could be mentioned, such as hydrogen-bonded bent-core materials (see work by Serrano et al., Zaragoza-Spain) or twist-bend nematogens (see work by Imrie et al., Aberdeen-UK).

Meta-extension of LC core is claimed with respect to the centre of mass situated at the aniline relevant aromatic ring in the Schiff based intermediate. It is clearly illustrated in fig-4. As per the reviewer's directive, other examples of supra-molecular HBLCs, Bent LCs exhibiting T_{NB} phases are also referred (Ref-52-57) in modified text (Introduction, 2nd paragraph in p-3; along with the Serrano et al and Imrie et al reports) in the list of references also.

Bullet point iii) has not been addressed in the text, but rather argued, in liaison of bullet point

Text regarding electro-negative O-atom to promote lateral stacking, and hence the predominant growth of layered smectic phases is introduced in section-3c, p-10, before

drawing conclusions. Reasoning for predominance of smectic phases is attempted for its connection to meta-extended core.

iv).Please refer more clearly in bullet point

Explanation for the observed quenching Nematic phase is written (1st paragraph of p-13), while the conclusion is written in p-17 & 18.

v) to the effect of “n” on the phase behaviour of the HBLCs, since, it was one of the main aims. This must include bullet point vii).

Appearance of quasi-2D phases with increasing flexible component ‘n’ is entirely different issue than that in bullet point-vii (of old version) regarding the realization of multicritical points. Hence, multicritical points and exotic symmetries) and orientational disorder by long chains are scribed in two different sentences. Text is re-written to bring proper connectivity between the appearance of exotic phases (in p-11, section-3dii) induced by long chain (increasing ‘n’) through orientational disorder, and multicritical points (p-13, section-3e) in whose vicinity rare symmetries converge.

Page 18. Line 12. Define “exotic” symmetries.

As suggested by reviewer, the explanation (p-13, in section-3e for Phase diagram, 3rd para-graph) for exotic symmetries and realization of multi-critical points is introduced.

As all the comments made by the reviewer are responded, answered and properly defended by reports of contemporary relevance, **revised script may be considered for publication.**

Figure-5

